SEMMELWEIS EGYETEM
DOKTORI ISKOLA

Ph.D. értekezések

3138.

KOPPÁNY FERENC

Fogorvostudományi kutatások
című program

Programvezető: Dr. Varga Gábor, egyetemi tanár
Témavezető: Dr. Németh Zsolt, egyetemi tanár

NANOMORPHOLOGICAL EXAMINATION OF TITANIUM SURFACES

PhD thesis

Ferenc Koppány

Károly Rácz Doctoral School of Clinical Medicine
Semmelweis University

Supervisor: Zsolt Németh, MD, med. habil.
Official reviewers: Bálint Molnár, DMD, Ph.D.
Márk Fráter, DMD, habil.

Head of the Complex Examination Committee: Gábor Varga, MD, D.Sc.

Members of the Complex Examination Committee:
Miklós Sárdy, MD, med. habil.
János Vág, DMD, med. habil.
András Folyovich MD, Ph.D.

Budapest
2024

Table of Contents

List of Abbreviations

- **AFM:** Atomic Force Microscopy
- **CaP:** Calcium Phosphate
- **CC:** Concentrated
- **CV:** Coefficient of Variation
- **DC:** Direct Current
- **HCl:** Hydrochloric Acid
- **HF:** Hydrofluoric Acid
- **HNO_3:** Nitric Acid
- **H_3PO_4:** Orthophosphoric Acid
- **NaOH:** Sodium Hydroxide
- **NP:** Nano-Pitted
- **NT:** Nanotubular
- **PSHA:** Plasma Sprayed Hydroxyapatite
- **Ra:** Arithmetical Mean Height
- **Rq:** Root Mean Square Deviation
- **ROI:** Region of Interest
- **Sa:** Surface Average
- **SEM:** Scanning Electron Microscopy
- **TiO2**: Titanium Dioxide
- **TPS:** Titanium Plasma-Spraying
- **XPS**: X-ray Photoelectron Spectroscopy

1. INTRODUCTION

The integration of dental implants into the body is a highly complex process involving both biomechanical and biological factors. The initial fixation is provided by mechanical anchorage, which is highly influenced by the shape of the implant. The result is usually referred as primary stability. Following insertion, the implant surface plays a secondary role, similar to a landscape to be populated by host cells and microbiota, that are also present at the time of implantation. [1, 2] The race for the surface begins during the wound healing process, where bonds of varying energy levels form between the surface and water molecules, ions, polysaccharides, and proteins. [3] Subsequently, bone-forming cells appear in the vicinity, and newly formed bone embeds the implant. This leads to a biomechanical anchorage, ususally referred as secondary stability or osseointegration. The literature demonstrates a progressive understanding of these phenomena, driven by the refinement of investigative techniques and advancements in biomaterials development. It became evidental that surface characteristics can directly enhance tissue cell attachment and proliferation, or inhibit bacterial colonization. This fuels surface science and surface modifications. Many methods already yield long-term clinical results and are commercially available, but the quest for the ideal implant surface is still in target range. Most studies, including this thesis, aim to translate findings from basic research towards clinical applications. The ultimate implementation relies on clinicians and practitioners to produce long-term, evidence-based data, establishing a broad timeframe for innovations to consequently outline their reliability. In order to present a more comprehensive perspective of my work, i would like to summarize the scientific background and interpretations of different phenomena related to dental implant surfaces.

1.1. Milestones in surface modifications

1.1.1. Titanium and Biocompatibility

Biocompatibility is not a property of just the material itself, but rather a property of how the material reacts with its environment. Historically, the absence of an adverse reaction was long considered as a main requirement for biocompatibility. [4] At the beginning of the 19th century, the need for improved strength, durability and corrosion resistance aligned with minimal adverse reactions arose, due to the increasing use of metals and other materials in medical applications. In 1951, *Per-Ingvar Brånemark*, a Swedish orthopedic surgeon, conducted experiments on rabbits, discovering that titanium could integrate with bone at the level of light microscopy by inducing minimal connective tissue reaction. [5] The scientific application of titanium as a biocompatible material in conjunction with osseointegration opened new possibilities in numerous areas of biomedicine, since it had a unique combination of biocompatibility, strength and resistance to corrosion [5]. Interestingly, the term biocompatibility and biomaterial were only defined in 1986, on a consensus conference. The statement defined biomaterials as "nonviable materials used in medical devices that interact with biological systems", and biocompatibility as "the ability of a material to perform with an appropriate host response in a specific application" [6, 7] The scientific significance of the congress was the understanding that biocompatibility involves not only the absence of harmful effects but also the positive interaction with the biological environment. Additional definitions were later added at the China 2019 conference. [8] This broadened the concept of biomaterials to include any substance that has been engineered to interact with living systems, specifically for therapeutic or diagnostic procedures in both human and veterinary medicine. The biocompatibility of titanium is due to the oxide layer that coats the metal surface and forms spontaneously, upon contact with oxygen from atmospheric air [9, 10] Maintaining the integrity of this layer is crucial during subsequent processing for dental purposes. Titanium was identified as an element by mineralogist William Gregor in Cornwall, Great Britain in 1791. German chemist Martin Heinrich Klaproth also verified the presence of an unknown element in an ore from Hungary in 1795. [11] However, it was not until the early 20th century that titanium began to be used in industrial applications. The method which is still the primary method today to produce commercial-grade titanium was invented by the american chemist William J. Kroll in the 1940s. Since titanium is rarely available in its pure form in nature, it is usually extracted from minerals through the reductive Kroll process, where the titanium is separated from the other elements and purified for use in various applications. Further processing of titanium resulted in various oxides and alloys and led to a big step forward in the vast majority of industrial fields in the second half of the 20th century.

1.1.2. Importance of Surface Roughness

The prototype for dental implants was created by *Brånemark* based on his own findings about osseointegration.[12, 13] These screw-type implants were made from commercially pure titanium and underwent no further surface treatment after being machined to size. Implants produced this way were the hallmark of modern implantology until the end of the eighties. After the clinical success of the first dental implants, and the ongoing research on surface properties, it became increasingly evident that surface roughness plays a crucial role in influencing osseointegration. [14] (Figure 1)

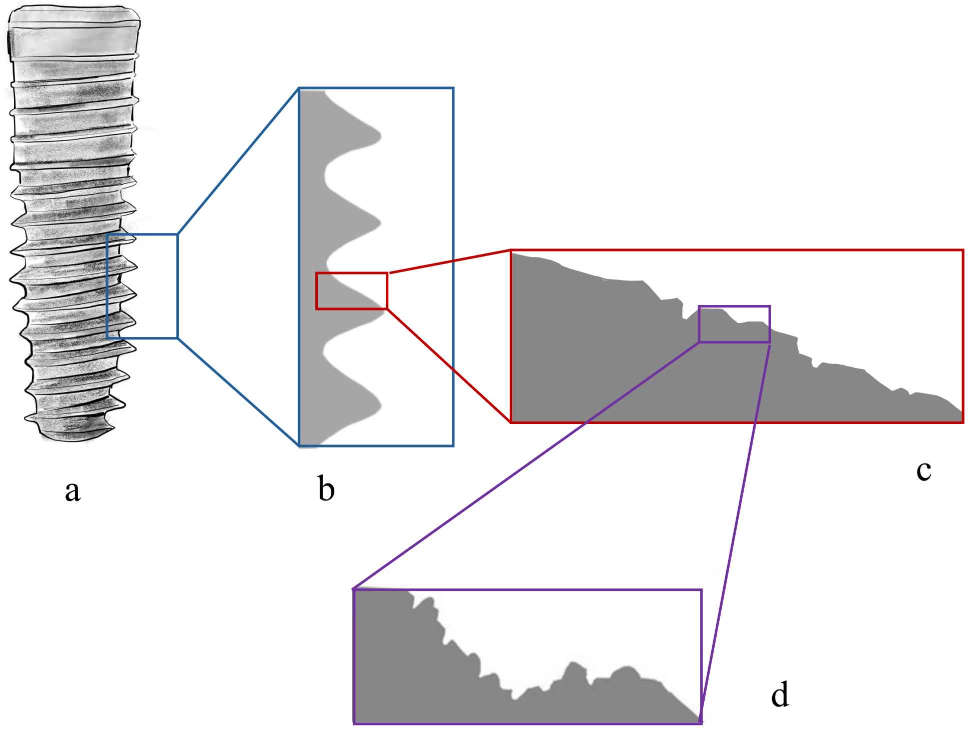

Figure 1. Implant macro level represented by the overall shape and thread design (a,b). Micro and nano structures are observed at higher resolution (c,d) (Source: personal implementation)

Among the first treatment methods to increase the surface area were grit blasting with titanium dioxide particles [15], titanium plasma spraying [16], and hydroxyapatite coating [17]. Clinically, roughened surfaces have shown faster healing compared to the smooth, machined surfaces. [18] *Esposito et al.* highlight that implants with rough surfaces generally exhibit a lower prevalence of early implant failures compared to machined implants, because bone apposition occurs more rapidly. However, they also note that this initial advantage diminishes over time, as there is a clear positive correlation between surface roughness and the rate of bacterial colonization on oral implants. [19, 20] Surface roughness characterization is associated with *Ann Wennerberg*. [21] She pointed out despite several authors reporting various results, that "there has been some confusion about what is rough and what is smooth". [22] Following her studies, surface roughness measurements were generally classified into smooth, minimally rough, moderately rough, and highly rough surfaces. Minimally rough surfaces (Sa=0.5-1 µm) exhibit better osseointegration compared to smooth surfaces (Sa=0-0.4 µm), and studies have shown that moderately rough surfaces (Sa=1-2 µm) promote better bone formation than highly rough surfaces (Sa>2 µm). [23] In light of these findings, a sandblasting combined with dual acid-etching procedure was developed. [24] Extensive literature and long-term clinical results consistently highlight this method and it has become pivotal in the production of contemporary commercially available dental implants and sets a reference in current surface research methods. [25-28] Various coatings, such as hydroxyapatite, bioactive glass, and recent cellular and molecular depositions have also been investigated for their potential use. While these coatings represent a specialized field of study, concerns about delamination, long-term stability and adverse effects remain relevant today. [29]

1.1.3. Paradigm shift

In the late 90s new conclusions were forming. [30] Besides surface topography and roughness parameters new properties, such as chemical composition and surface energy have been reported to influence interfacial reactions of a biomaterial. [24, 31] *Schwartz and Boyan* outlined a paradigm shift from focusing solely on bone apposition and adverse reactions as determinants of biocompatibility to a broader consideration of tissue responses. They noted that, although biocompatible materials do not cause significant adverse reactions or immune rejection, they still elicit a wide range of tissue responses. Consequently, the emphasis should shift from merely understanding the mechanisms of bone formation to a more comprehensive study of the overall wound healing process. [32]. This wound healing paradigm encompasses serum protein conditioning, the acute inflammatory response with clot formation and release of wound healing factors, recruitment of undifferentiated mesenchymal cells to the surface, their attachment, proliferation, osteoblastic differentiation, followed by matrix vesicle production and maturation, and calcification. [33-35] *Rupp et al*. also described the shift of interest from the mechanical surface characteristics to the physico-chemical surface properties, underlining the importance in substrate-protein reactions. He also emphasized the role of hydrophilicity in the early and subsequent bacterial colonization. [9] Several later studies also undeline the importance of surfaces roughness, highlighting that it not only enhances bone cell adhesion by increasing the interlocking area but also positively influences cellular activities. [23, 36] Subsequent studies have confirmed this hypothesis, showing that Ti implants with biomimetic osteoclast resorption pit surfaces promote the differentiation of macrophages into a pro-healing M2 pathway, while smoother surfaces tend to lead to a pro-inflammatory M1 phenotype. [37, 38] This suggests that the surface topography of Ti implants plays a crucial role in directing the immune response, with biomimetic designs favoring healing and smoother surfaces potentially triggering inflammation. Histopathological analysis of tissues confirms that this effect occurs in vivo as well. Implant properties, including biomimetic topographies, also influence adaptive immune cells, maintaining the immaturity of dendritic cells and modulating T cell and helper cell activation in response to surface topography and wettability. [37, 39] As the importance of surface characteristics besides surface roughness was beeing extensively studied, researchers in the late 1990s began to investigate the effects of nanoscale surface irregularities on alloplastic materials.

1.1.4. Recent focus

Numerous studies followed *Webster et al*. findings on osteoblasts behaviour on nanophase ceramics. He sintered hydroxiapatite grains, smaller than 100 nm, on ceramic surface [40] He demonstrated that hydroxyapatite nanotopology enhances osteoblast proliferation and the synthesis of alkaline phosphatase. Also, deposition of calcium containing mineral has been observed. Following the paradigm shift from bone formation to wound healing, *Webster's* research brought nanorough surfaces to the forefront, providing a new focus on cellular interactions. Since then, studies on creating nano topography for implants have multiplied. The presence of intentional nanometer-scale features is theoretically expected to enhance the bone-to-implant response [41-43].

However, it is speculated that unintentional nanotopography may not have controlled biological effects, as heterogeneous nanostructures can form due to the natural oxidation of the titanium substrate. [42] These factors influence cellular behavior by interacting with proteins, modulating immune responses, and affecting chemical signaling pathways. [44-47] Moreover, nanoscale roughness can impart antibacterial properties to the implant surfaces [48], reducing the risk of infections with a possible impact of improving overall implant success [49].

1.2. Nanoscale surfaces

By the early 21st century, it became widely accepted that surface modifications at any scale enhance bone response by improving the initial interaction between the implantable device and host biofluids. Additionally, it was understood that the surface of an implant is inherently different from its bulk material. [50-53] The advancements in nanoscience and nanotechnology also found nanoscale (1 nm to 100 nm) to be a magical point on the dimensonal scale, [54] which is due to the changes how materials behave according to quantum mechanical relationships. In bulk materials, the energy levels of electrons are continuous, because the large number of atoms cover all energy levels. By shrinking the size of the material, the energy levels become more and more discrete and quantum effects become prominent. In other words, in nanoscale materials (1-100 nm) an electron in an atom can only occupy certain energy levels, and it must absorb or emit energy in discrete amounts (quanta) to move between these levels. This effect is not significant going from macro to micro dimensions but becomes dominant when the nanometer size range is reached. [55, 56] These quantum structures are physical structures (Table 1) where all the charge carriers are confined within the limited physical dimensions. [57, 58] Quantum confinement effects can cause nonmagnetic materials such as palladium, platinum, and gold to become magnetic at the nanoscale, and these effects can also result in significant changes in electron affinity, which directly enhances the catalytic properties of materials. [59] Based on my literature research, I assume that this quantum effect can not only occur when the size of the materials fall into the nanometer range, but also in case of nanomorphological patterns as well. This assumption might propose an interesting area of research in an interdisciplinary approach.

Table 1. Most commonly investigated nanostructures, related surface treatment methods and possible applications. (Source: Table compiled by the author of this thesis)

Nanostructure	Material	Method	Application
Nanotubes	TiO_2	Anodization	Experimental optimization
		Hydrothermal treatment Anodization	Implant material Bone regeneration
	TiO_2 Hydroxyapatite	Electrochemical treatment	Dental implants
Nanoparticles	Silver and hydroxiapatite nanoparticles	Electrodeposition	Antibacterial property Implant material
Nanowires	Zn-Ti	Acid etching Chemical treatment	Biocompatibility and antibacterial activity Implant material
Nanopores	TiO_2	Chemical and electrochemical treatment	Biological integration Dental implants

Nanotechnology also enables the impartation of structures that mimic the architecture of living tissues, inducing varied responses in different biological environments. [60-65] In summary, advancements in nanotechnology related to dental implant research have demonstrated that larger surface areas and higher surface-to-volume ratios generally increase the reactivity of nanomaterials due to the greater reaction surface. [66] Additionally, these properties significantly influence the surface properties of the materials. [62, 67]. Looking from a manufacturing perspective, reduced scale manufacturing techniques allow any nanometer scale features patterning on implant surfaces. [62, 68]. However, since high throughput is necessary for economically viable implant surface manufacturing, industrial methods for nanometer scale surface modification are restricted to a reduced number of additive and subtractive methods. The most common nanoscale related methods in conjunction with dental related research are shown in Table 2.

Table 2. Techniques for the addition of nanotechnology to dental implants. [69] (Source licensed under Creative Commons CC BY-NC).

Methods	Characteristics
Self-assembly of monolayers	The exposed functional end group could be a molecule with different functions (an osteoinductive or cell adhesive molecule).
Compaction of nanoparticles	Conserves the chemistry of the surface among different topographies. Not readily applied over implant surfaces.
Ion beam deposition	Can impart nanofeatures to the surface based on the material used.
Acid etching	Combined with other methods (sandblasting and/or peroxidation) can impart nanofeatures to the surface and remove contaminants.
Peroxidation	Produces a titania gel layer. Both chemical and topography changes are imparted.
Alkaline treatment (NaOH)	Produces a sodium titanate gel layer allowing hydroxyapatite deposition. Both chemical and topographic changes are imparted.
Anodization	Can impart nanofeatures to the surface creating a new oxide layer (based on the material used).
Sol-gel (colloidal particle adsorption)	Creates a thin-film of controlled chemical characteristics. Atomic-scale interactions display strong physical interactions.
Discrete crystalline deposition	Superimposes a nanoscale surface topographical complexity on the surface.
Lithography and contact printing technique	Various materials and forms can be used to cover the surface. Approaches are labor-intensive and need to be developed extensively before being applied to implant surfaces and being translated for clinical use.

1.2.1. Microrough Surfaces with Nanoscale Modifications

Since nanoscale roughness is inherently present on most surfaces, dental implant manufacturers started to emphasize these topographical features on their existing product lines. Subsequent scientific evaluation of the most common implant brands revealed nanofeatures on many of them, such as SLActive (Straumann Institute, Basel, Switzerland), OsseoSpeed (Astra Tech Implant System, Dentsply, Germany), NanoTite (3i/Biomet, Florida, USA) and TiUnite (Nobel Biocare, Bern, Switzerland) surfaces. However, the density and appearance may vary. [70] Since, the benefits of moderatley rough surfaces have already been clinically proven, many researchers suggest, that nanoscale surface elements on top of micro-level topography can be beneficial in the long-term success. [71, 72] *Ehrenfest et al.* did an extensive study on commercially available dental implants regarding the presence of micro and nanoscale roughness. [73] His findings are summerized in Table 3. Most surfaces reviewed in this study utilized commercially pure titanium as core material. The surface modification methods applied theoretically could enable nanoscale patterning, however only four products out of 14 showed distinctive nanoscale roughness. Regarding these four implants, two of them showed heterogenous appearance based on nanoparticles while the other two showed extensive nanoroughness in homogenic distribution. The homogenous nanoroughness was achieved by blasting with TiO_2 and hydrofluoric etching in one case and blasting was followed by unkown post processing in the other case. Nonetheless, these latter methods showed the highest degree of surface cleanliness. The authors note that implant surfaces often exhibit heterogeneity due to inconsistencies in surface characteristics, uncontrolled crystal clusters, and various types of surface contamination. To assist practitioners in making informed decisions and improving healthcare outcomes, the authors advocate for the development of a classification system for implant surfaces. [73]

Table 3. Surface characteristics of commercially available dental implants. [73] (Table created by the author of this thesis based on the cited article.)

BASIC PROCEDURE	SURFACE NAME	ADDITIONAL METHODS	SURFACE ELEMENTS	SURFACE CHARACTERISTICS
Anodization	TiUnite	High quantity of calcium and phosphorus added chemically	phosphorus, fluoride, sulfate	Microporous, smooth on nanoscale, extended cracks
	Ospol	Low quantity of calcium and phosphorus added chemically	calcium and phosphorus, sodium	Microporous, smooth on nanoscale, small local cracks
Titanium Plasma-Spraying (TPS)	Kohno HRPS	N/A	Phosphorus (as phosphate), fluoride, sulfur (as sulfate)	Maximal microroughness, smooth on nanoscale, many extended cracks
Blasting/Etching	Osseospeed	Blasting with TiO2, etching with hydrofluoric acid	Residual level of fluoride, no polliution	Moderate microroughness, extensive nanoroughness
	Ankylos	Blasted/etched with alumina particles	Alumina (Al2O3), sodium, fluoride, calcium, phosphate, zinc, chloride, sulfur (as sulfate)	Moderate microroughness, nanosmooth, heterogeneous
	Zimmer MTX	Blasting with hydroxyapatite on grade 5 titanium	Calcium phosphate (CaP), significant silicon	Minimal microroughness, nanosmooth, homogeneous
	Camlog Promote	Blasted/etched	Zinc, calcium	Moderate microroughness, nanosmooth, homogeneous
	BTI Interna	Etched	High levels of organic carbon species	Aggressive etching pits, smooth on microscale and nanoscale
	EVL Plus	Blasted/etched	Residual calcium phosphate, alumina (Al2O3) particles, residual fluoride	Minimal microroughness, nanosmooth
	Twinkon Ref	Blasted on grade 5 titanium	Calcium, alumina (Al2O3), thick organic carbon, silicon, sulfur (as sulfate), chloride, zinc	Minimal microroughness, nanosmooth, heterogeneous
	Ossean	Blasted/etched, unknown postprocessing	Low levels of calcium phosphate, no pollution	Minimal to moderate microroughness, nanoroughness, homogeneous in chemistry and topography
Blasting/Etching with coating	3I NanoTite	Etched on grade 5 titanium, CaP coating	CaP particles, traces of fluoride and sulfur	Smooth and flat microroughness, significant nanotexture, heterogeneous due to varying CaP particles
	SLActive	Blasted/etched, NaCl physiological solution	NaCl crystals, traces of fluoride, potassium, calcium, phosphate	Moderately rough and rugged microtopography, significant nanotexture, heterogeneous due to NaCl aggregates
	Integra-CP	Blasted/etched, CaP ion-beam assisted deposition	Thicker CaP coating (>100 nm), traces of fluoride and sulfur	Flat microscale, smooth nanoscale

Due to the growing number of investigations some concerns have been made and further studies are required to achieve an ideal surface. For example, in case of titanium plasma-spraying (TPS) can increase the implant's surface area up to six times. However, concerns include potential delamination at the implant-coating interface and titanium particles found in adjacent bone. [74] In case of plasma sprayed hydroxyapatite (PSHA), which is commonly used for calcium phosphate coatings, the interface with titanium often has weak mechanical resistance, leading to potential implant failures and inflammatory responses due to particle release. Consequently, PSHA-coated implants have become less popular in dental practice, as studies have shown that the coatings do not degrade uniformly over long periods, compromising their long-term effectiveness. [74] To improve these methods efforts are being made to change the manufacturing parameters but there are usually more concerns with coatings in relations with biocompatibility due to delamination effects. [75] The formation of an ideal surface incorporating new insights is still relevant. There is a trend to create homogenized surfaces which esnures consistent surface behaviour. *Zhang* emphasizes regarding future perspectives: "The next generation of dental implants will employ optimized nanotopography to simultaneously augment antibacterial and osseointegration functions." He also adds that "it remains difficult to fabricate uniform nanostructures rapidly and on a large scale." [76]

1.3. Insights of anodization

According to my literature research i found anodization as one of the most promising methods that has received a lot of interest for dental implant surface modification [69, 77-80]:

- the method is capable of imparting both micro- and nanoscale elements in a homogenous distribution
- anodization thickens the oxide layer while desired patterns can be achieved (nanotubes, nanopits)
- anodized surfaces have shown bioactivity
- some of the resulting surfaces have already been clinically proven biocompatible
- technologically simple and cost-effective

This surface modification technique is an electrochemical method that deposits an oxide layer on the anode surface of a metal substrate. It uses an electric field to ionize elements in the aqueous electrolyte and facilitate their diffusion to the metal, as illustrated in Figure 2. [77]

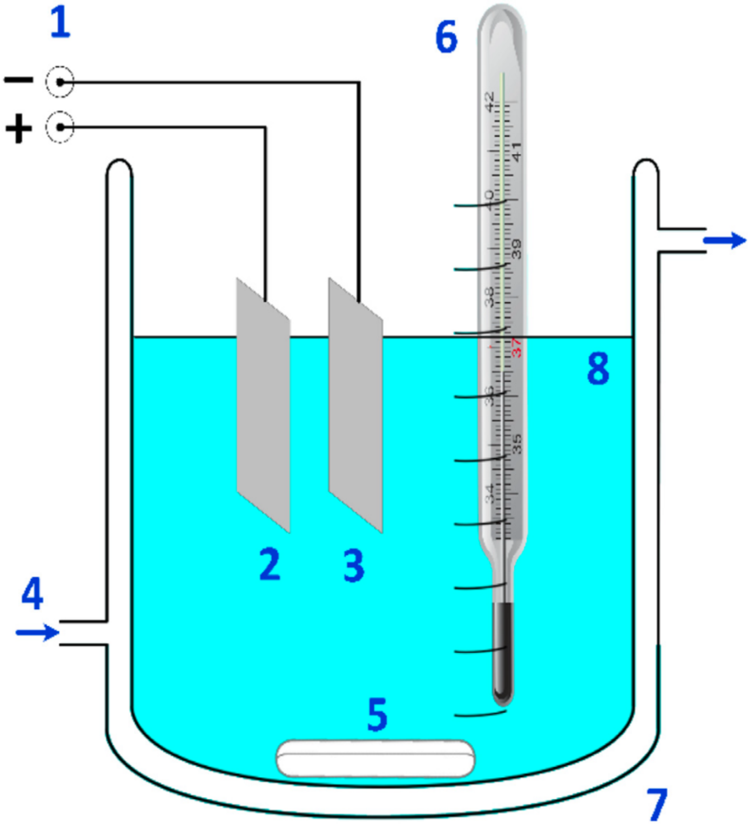

Figure 2. Schematic diagram of anodic oxidation, AO electrochemical cell: (1) power supply, (2) anode (3) cathode (4) cooling water (5) magnetic stirrer bar (6) thermometer, (7) jacketed beaker, (8) electrolyte [77] (Source licensed under Creative Commons CC-BY-NC-ND).

By adjusting electrochemical parameters such as applied voltage, electrolyte composition and concentration, and current density, the formation of anodized titanium with specific properties can be controlled. Additionally, various compounds, such as calcium phosphate (CaP), can be incorporated into the titanium surface when anodized in CaP-containing electrolytes. Today, titanium-based devices doped with CaP compounds are widely used in clinical applications, including dental and orthopedic implants. [77] With the anodizing process, it is also possible to produce tubular orientation of TiO_2. These are cylindrical nanostructures that are vertically oriented and hollow. The electrochemical growth behavior and surface oxide properties are controlled by several process parameters, including nature of the substrate, forming voltage, electrolyte related parameters (ion content, concentration, temperature, pH the current density, the distance between the anode and cathode), and circulation speed. [81] The formation of TiO_2 nanotubes (TNTs) typically occurs under potentiostatic conditions with an applied voltage of less than 30 V. The growth mechanism of TiO_2 nanotubes is illustrated in Figure 3. The length of the nanotubes is determined by the equilibrum state between electrochemical oxidation and electrochemical corrosion. [77]

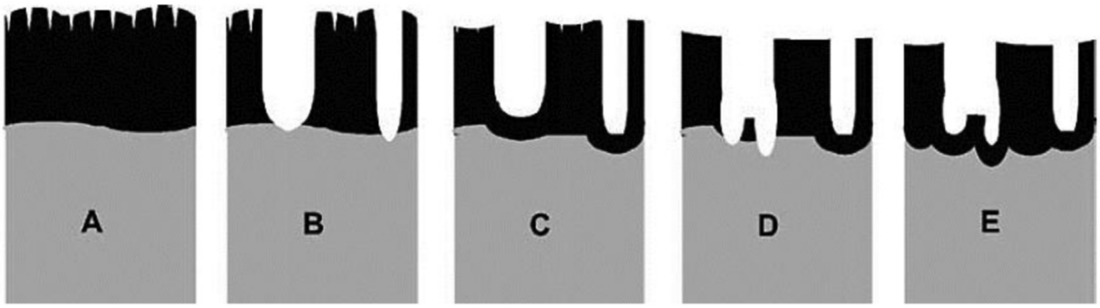

Figure 3. TiO_2 layer forms on the anode (A). Fluoride ions then react with this newly-formed TiO_2, creating irregular pits on the TiO_2 layer (B). As anodizing progresses, the pores become uniformly distributed and well-structured within the oxide layer (C). The depth of these pores continues to increase due to ongoing electrochemical oxidation and corrosion (D). Eventually, TiO_2 nanotubes are fully formed (E). [77] (Source licensed under Creative Commons CC-BY-NC-ND).

Since nanotubes offer surface properties that can enhance cell-bone adhesion of dental and othopedic implants, they are in focus of many studies [65, 69] In addition, nanotubes can also be filled with antibacterial medicines to prevent infections. [82, 83] *Weszl et al.* investigated the mechanical and chemical properties of nanotubular (NT) and nano-pitted (NP) anodic films on grade 2 titanium surfaces. [84] Nanopits are depressions or pits on the surface, also created through anodization but with a different parameters. They are not hollow like nanotubes but rather indentations on the surface. Their study found that while NT films were highly sensitive to process parameters and prone to corrosion and exfoliation, NP films demonstrated high reproducibility and mechanical integrity. The NP design exhibited superior corrosion resistance, maintained its structural integrity under mechanical stress, and had consistent surface characteristics compared to NT films, which showed higher concentrations of fluorine dopants leading to poor adhesion and increased exfoliation. These findings highlight the potential of NP anodic films for enhancing the durability and biological performance of titanium implants. [84] Notably, NP films not only exhibit improved mechanical strength but also enhance osseointegration and demonstrate significant antibacterial effects, which are crucial for preventing implant-related infections and ensuring successful integration with bone tissue. [85] Anodised titanium may appear in different colours, and this phenomenon is called colourisation. The cause of different colours in anodised titanium depends on the thickness and the crystal structure of the anodic TiO_2 layers. *Mühl et al.* compared machined surfaces with anodized surfaces to investigate subsequent soft tissue integration. Interestingly, the anodization parameters were selected to produce a pink-colored surface, which enhances the aesthetic appearance of implant abutments by contributing to a more aesthetically pleasing appearance. [86]

1.4. Surface characterization

Surface treatment methods induce a range of irregularities on surfaces and quantitative data, such as surface roughness provides a numerical description of a surface texture. According to *Wennerberg et al.*, many researchers confuse the concept of surface topography with the concept of surface morphology. Surface topography is a broad term that includes the overall shape of the implant, involving millimeter-scale geometric alterations, the waviness of the surface at the scale of a few hundred micrometers, and the roughness, which encompasses surface features smaller than a hundred micrometers. [21]

1.4.1. Quantitative Analysis

Various techniques are employed to analyze surface roughness, which can be measured in macro, micro, and nano ranges as well.

Surface Roughness

The universally investigated parameters are:

- **Ra** (**R**oughness **a**verage - profile roughness) is the arithmetic average of the deviations of the peaks from the ideal smooth surface and involves two dimensions.

- **Sa** (**S**urface **a**verage - area roughness) measures the average absolute deviation of the examined surface area from the ideal smooth surface, thus involving three dimensions.
- **Rq** (root mean s**q**uare **R**oughness) is the root mean square average of the deviations of the surface profile from the mean line.

Increasing surface roughness also promotes bacterial adhesion and biofilm formation which can jeopardize the integration and long-term retention of implants. [87] The structural characteristics of the extracellular matrix are on a nanometer scale, and biomaterials that mimic this environment can more effectively support bone regeneration processes.[71] *Matinlinna et al.* indicates that surface roughness values are useful as a guideline for comparison, but not an absolute value to determine the ability of osseointegration. [88] The most common investigation methods of surface roughness are scanning electron microscopy (SEM), optical profilometry, atomic force microscopy (AFM) and contact angle measurement.

Scanning Electron Microscopy (SEM)

A scanning electron microscope (SEM) uses a focused beam of high-energy electrons to scan a sample surface. The electron beam, directed by deflection coils, interacts with the sample, producing signals like secondary electrons and backscattered electrons. These signals are captured by detectors to form high-resolution images and compositional maps of the surface. The beam's raster pattern aligns with the image pixels, providing detailed 2D views of surface morphology and composition. [89, 90]

Optical Profilometry

An optical profilometer uses a light source, like a laser or white light, to illuminate a sample surface. It operates on interferometry, splitting the light into two paths: one reflects off the sample and the other off a reference mirror. The combined reflections create an interference pattern, indicating surface height variations. An objective lens focuses the light, and controlled movements scan the surface. The data generates high-resolution 3D maps, providing detailed information on surface roughness, texture, and topography. [91]

Atomic Force Microscopy (AFM)

Atomic force microscopy (AFM) is a high-resolution technique for analyzing surface topography at the nanoscale. It scans a sharp tip across a sample's surface, measuring the forces between the tip and the sample to produce detailed 3D images. The setup includes a cantilever with a sharp tip, which deflects due to forces like van der Waals, electrostatic, and chemical bonding. A laser beam reflects off the cantilever onto a detector, tracking vertical movements to generate a topographical map. AFM operates in different modes: contact, tapping, and non-contact, adjusting the cantilever height to maintain consistent scanning conditions. [92]

Contact Angle Measurement

A contact angle measurement uses a liquid droplet, typically water, to evaluate the wettability of a sample surface. The term refers to the characteristic of a given material allowing liquids to adhere to its surface. (Figure 4).

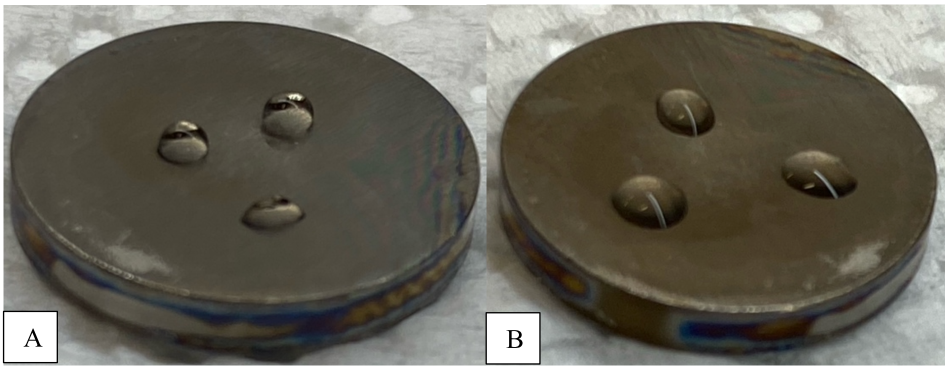

Figure 4. Surfaces with varying wettability. Due to surface tension, water droplets may either remain elevated on hydrophobic surfaces with lower wettability (A) or spread out more on hydrophilic surfaces with higher wettability (B). (source: personal)

Contact angle measurements operate based on the principle of surface tension. The liquid droplet is carefully deposited onto the sample surface using a precise dispensing system, such as a syringe or pipette. The contact angle is defined as the angle formed between the tangent to the liquid droplet surface and the solid surface at the point of contact. This angle depends on the balance of adhesive forces between the liquid and the solid and cohesive forces within the liquid, which correlate to the wettability of the surface. The system illuminates the droplet from the side to create a clear profile of the liquid-surface interface. A high-resolution camera captures an image of the droplet. The contact angle is then measured using software that analyzes the droplet's shape and calculates the angle formed at the point of contact with the surface. The processed data is used to determine the contact angle, which provides quantitative information about the surface's hydrophilicity or hydrophobicity. Lower contact angles indicate better wettability, while high contact angles indicate poor wettability. The surfaces can be marked as hydrophilic if the contact angle is between 0-90 degrees and hydrophobic if the contact angle is above 90 degrees. [93]

1.4.2. Qualitative Analysis

Surface qualitative properties refer to the characteristics of a surface that describe its chemical composition, chemical state, surface energy and other attributes that affect its interaction with the environment. Common method to describe elemental composition and surface energy are X-ray photoelectron Spectroscopy (XPS). [94, 95] Since cells interact with implant surfaces at the nanoscale level, the recognition of these properties are becoming increasingly important.

XPS

The surface of an implant is inherently different from the bulk material. The degree of crystallinity, chemical composition, and presence of desired or undesired elements are properties that frequently are different, comparing the surface with its bulk. XPS utilizes a monochromatic X-ray source, commonly aluminum (Al Kα, 1486.6 eV) or magnesium (Mg Kα, 1253.6 eV), to irradiate the sample. These sources provide the necessary energy to eject core electrons from the sample, enabling the measurement of their binding energies. Atoms have electrons arranged in different energy levels or shells (K, L, M, etc.). The K shell is the innermost shell, followed by the L shell, M shell, and so on. When an electron in the K shell is ejected (for instance, due to the interaction with an external high-energy photon), it leaves behind a vacancy. An electron from a higher energy level (like the L shell) can fill this vacancy. The transition of an electron from a higher energy level (L shell) to a lower energy level (K shell) releases energy in the form of an X-ray photon. This emitted X-ray is known as a characteristic X-ray because its energy is characteristic of the difference in energy between the two shells involved in the transition. [96]

1.5. The role of wettability

Wettability seem to play an important role in dental implant surfaces because it greatly affects the initial interactions between the implant and the biological environment. [37, 97] A higher wettability enhances protein adsorption, which is essential for the adhesion and proliferation of osteoblasts. This improved cell adhesion leads to better osseointegration, ensuring the stability and longevity of the implant. Additionally, surfaces with optimal wettability can reduce bacterial colonization, minimizing the risk of infections. [52] Therefore, considering wettability in implant design is vital for enhancing the overall success and functionality of dental implants. [98] Hydrophilic surfaces generally provide better fluid transport at the implant-tissue interface. By forming an even fluid film, they can enhance cell proliferation and differentiation. The increased surface energy influences interactions between tissue proteins and the implant surface, accelerating clot formation and initial healing processes. The hydrophilic property increases the number of immune cells involved in wound healing, which may help reduce bacterial biofilm formation. According to studies, hydrophilic surfaces preserve the arrangement and function of proteins, whereas hydrophobic surfaces appear to induce denaturation. [52, 99] Literature shows that wettability enhances the beneficial biological effects that nanostructured surfaces provide regarding osseointegration. *Elias et al.* investigated complex surfaces with roughened topography and varying wettability, highlighting the importance of surface hydrophilicity. In a 12-week rabbit tibial model, anodized surfaces, which had the lowest roughness and highest hydrophilicity, showed the highest removal torque. This suggests that hydrophilicity may have a stronger impact than roughness alone. Notably, only anodized surfaces displayed well-defined nanostructures and had a statistically significant ($P < 0.05$) lower contact angle with water and NaCl, indicating greater hydrophilicity. [99] Other authors also report that anodized samples represent a significantly more hydrophilic surface than the turned ones. [86]

2. OBJECTIVES

Surfaces with nanotopography appear promising in terms of implant surface treatments. Their outstanding osseointegration potential and antibacterial effects can contribute to the long-term success of dental implants. The main goal of our study was to increase the hydrophilic property on a surface with nanotopographical features through acid etching while preserving its structural characteristics.

2.1. Specific aims

Our specific aims were:

-To produce a nano-pitted structure
-To apply various etching procedures
-To evaluate the result of etched surfaces
-To investigate the surface characteristics of most favourable etched surface
-To compare the wettability of the different etched surfaces

2.2. Null Hypotheses

$H0_1$: The applied etchants and parameters do not induce any changes in the properties of nano-pitted titanium oxide surfaces.

$H0_2$: The applied etchants and parameters result in similar surface roughness on the nano-pitted structure.

$H0_3$: The applied etchants and parameters do not induce significant changes in the hydrophilicity of the nano-pitted titanium oxide surface.

3. MATERIALS AND METHODS

3.1. Production and preparation of samples

Grade 2 titanium rods (Bibusmetals, Hungary) were purchased and machined into discs of 2 mm thickness and 14 mm in diameter. The discs were thoroughly cleaned in a two-step cleaning process followed by full drying after each step [100]:

1. ultrasonic cleaning bath in acetone (Molar Chemicals, Hungary) for 5 minutes at room temperature
2. drying at room temperature
3. washing in the ultrasonic cleaner using absolute ethanol (Molar Chemicals, Hungary) for 5 minutes at room temperature
4. drying at room temperature

3.1.1. Applying nano-pitted (NP) TiO_2 surface treatment

Nano-pitted (NP) TiO_2 surfaces were created using a protocol that was published previously by certain members of our research group. [84] Following this protocol, the titanium discs were briefly subjected to a three-step surface treatment process. [100]

1. **Electrochemical polishing to remove the machining marks**. A two-electrode setup was used with a reference electrode made of platinum. The electrolyte (NANOTI EP Electrolyte, NANOTI Ltd., Sutton Coldfield, UK) was driven by a DC power source (Elektro-Automatik, EA-PS8080-40) to create the potential difference between the electrodes. The velocity of the steady electrolyte flow (0.1 L/min) was maintained by using a thermoplastic mag drive centrifugal pump (HTM6 PP, GemmeCotti). The temperature of the electrolyte was kept at 15 °C. The applied current was 30 V for 35 seconds.
2. **Acid etching of the polished discs** was performed in an ultrasonic bath for 3 min at room temperature. This step is important to initiate the formation of hydroxide islands on the surface to catalyze nanopore formation. The compound applied

consisted of 0.1 wt% hydrofluoric acid (HF), 1 wt% orthophosphoric acid (H_3PO_4), and distilled water (Molar Chemicals, Hungary).

3. **Anodic oxidation was performed in to steps to grow NP anodic film on the surface**. An electrochemical reactor with a two-electrode setup (anode-cathode distance = 5 mm) was used that was driven by a continuous direct power supply (Elektro-Automatik, EA-PS 8360–15 2 U). The first step was performed using hydrofluoric acid at 20 V (DC) voltage for 3 min. The second step was carried out by applying hydrochloric acid at 14 V (DC) voltage for 1 min.

3.1.2. Application of various etchants

The discs with NP TiO_2 surface were further processed by using various etchants**.**

The chosen disc samples showed proper anodization results to be subjected for experiment. Based on the literature review four test groups were formed that were further treated with different etchants and identical etching parameters (Table 4). [100]

Table 4. The process of sample preparation. Altogether, four test groups were prepared by etching the NP surfaces using various acids. [100]

Workpiece	**NP TiO_2 Disc**			
Etchant	Dilute orthophosphoric acid	Concentrated orthophosphoric acid	Dilute nitric acid	Concentrated nitric acid
Etchant composition	(1 g 85 wt% H_3PO_4 + 98.9 g dist. H_2O)	(85 wt% H_3PO_4)	(1 g 65 wt% HNO_3 + 98.9 g dist. H_2O)	(65 wt% HNO_3)
Test group name	NP + H_3PO_4	NP + ccH_3PO_4	NP + HNO_3	NP + ccHNO_3
Etching time	3 min			
Etching temperature	20–60 °C			
Agitation	None.			
Cleaning Step 1 Step 2 Step 3	Rinsing in ultrasonic bath: In distilled for 4 min at room temperature. In acetone for 5 min at room temperature. In absolute ethanol for 5 min at room temperature.			
Storage of samples	In hermetically sealed containers			

3.1.3 Experimental groups

Five experimental groups (one control and four test groups) were created to investigate the effect of various etchants on the physicochemical properties of NP surfaces. As a control, untreated NP surfaces were used in the study. In each experimental group, one sample was tested. On each sample three regions of interest were randomly selected where the contact angle and optical measurements were carried out. The robustness of the surface treatment method justified the low sample number in the experiment [84, 100]

3.2. **Investigation of surfaces**

3.2.1. Scanning electronmicroscopy (SEM)

The surfaces of the test groups were investigated with Philips XL-30 ESEM electron microscope to evaluate the homogenity achieved by the various etchants. [100]

3.2.2. Optical profilometry

Bruker Contour GT-K0X optical white light profiler was used to measure the surface roughness of the 5 experimental groups. An 800 × 600 μm^2 size region of interest (ROI) was randomly selected on each sample. The arithmetical mean height (Ra) and root mean square deviation (Rq) values were measured on the samples. [100]

3.2.3. Contact angle measurement

Distilled water was used as test fluid for contact angle measurement on the surface of the samples using a drop shape analyzer (Krüss DSA25, Hamburg, Germany). The measurement started immediately seconds after dropping, the drop volume was 3 ± 0.3 µL. The Elipse (Tangent-1) fitting method (Advance software, Krüss, Hamburg, Germany) was used to determine the left and right contact angles of the drop. One drop was added per sample and the contact angle of this drop was determined by 35 measurements. The mean of these measurements characterized the contact angle of the sample. [100]

3.2.4. Atomic force microscopy

A Bruker Dimension Icon AFM was used to confirm the results of the optical profilometry. AFM measurements were performed in tapping mode using a Tap300Al g tip. The measurements were performed on the surface areas where obvious surface flaws did not appear. The measurements were performed alongside the full diameters of the discs. The arithmetical mean height (Ra) and root mean square deviation (Rq) values were measured on the samples. [100]

3.2.5. X-ray photoelectron spectroscopy

The reference (NP) and the most hydrophilic samples were also studied using X-ray Photoelectron Spectroscopy (XPS). The XPS instrument used in the study was a custom-built system using Mg Kα radiation from a Thermo Fisher XR4 dual anode X-ray source and a Specs Phoibos 150 hemispherical energy analyzer to measure the energy distribution of the photoelectrons. The background pressure in the analytical chamber was 2×10^{-9} mbar, but it rose to 4×10^{-9} mbar during the measurements due to the degassing of the samples. Due to the oxide coverage on the surface, a small amount of charging was also observed. This was corrected based on the position of the adventitious carbon peak. After recording the surface spectra, each sample was subjected to 3 keV Ar^+ ion-beam sputtering from a custom-built ion source for 10 min. The sputtering speed (calibrated on SiO_2) was 30 nm/h. This removed roughly 5 nm from the surface of each sample. Subsequently, a set of new XPS spectra were recorded to compare the composition of the surface to deeper layers. [100]

3.3. **Statistical Analysis**

The mean, standard deviation, and coefficient of variation were used from the descriptive statistics. The coefficient of variation (CV) is the normalized standard deviation (standard deviation divided by the mean). The CV value under 10% means a homogenous dataset, between 10 and 20% means a low heterogenous dataset, and between 20 and 30% means a very heterogenous dataset. Above 30%, the dataset is very volatile. [100]

A Kruskal–Wallis test was performed to compare the samples ($p < 0.05$) and a Games-Howell test for the post hoc comparison. The Games-Howell test was deliberately selected for post hoc analysis because it was nonparametric, unlike the Tukey’s test, as it did not assume equal sample sizes and homogeneity of variances. [100]

4. RESULTS

The results showed that the treatment with various etchants did not cause any apparent changes to the NP surface in terms of surface roughness (Table 5).

Table 5. Surface roughness of samples measured using optical profilometry. Ra: arithmetical mean height indicates the average of the absolute value along the sampling length; Rq: root mean square deviation indicates the root mean square along the sampling length. [100]

Treatments	**Surface Roughness**	
	Ra (nm)	**Rq (nm)**
NP	149	191
NP + HNO_3	153	199
NP + ccHNO_3	126	166
NP + H_3PO_4	137	178
NP + ccH_3PO_4	196	249
Average	152.2	196.6
Standard deviation	26.7	31.9
Median	149	191

Regarding Ra, the surface roughness of the of samples remained in the range from 126 nm to 196 nm with an average of 152.2 nm (±26.7 nm) and a median of 149 nm. Regarding Rq, the surface roughness values of the of samples ranged from 166nm to 249 nm with an average of 196.6nm (±31.9 nm) and a median of 191 nm. [100]

Scanning electronmicroscopy showed that more aggresive etchants revealed definitive grain borders in the crystalline structre. (Figure 5) This refers to changes in the crystalline structure, which can lead to varying local surface energies affecting overall surface wettability and material behavior. [101] The results showed that concentrated and dilute H_3PO_4 treatment resulted in a relatively homogenous structure compared to both dilute and concentrated HNO_3, but the border lines were detectable in case of each etchant.

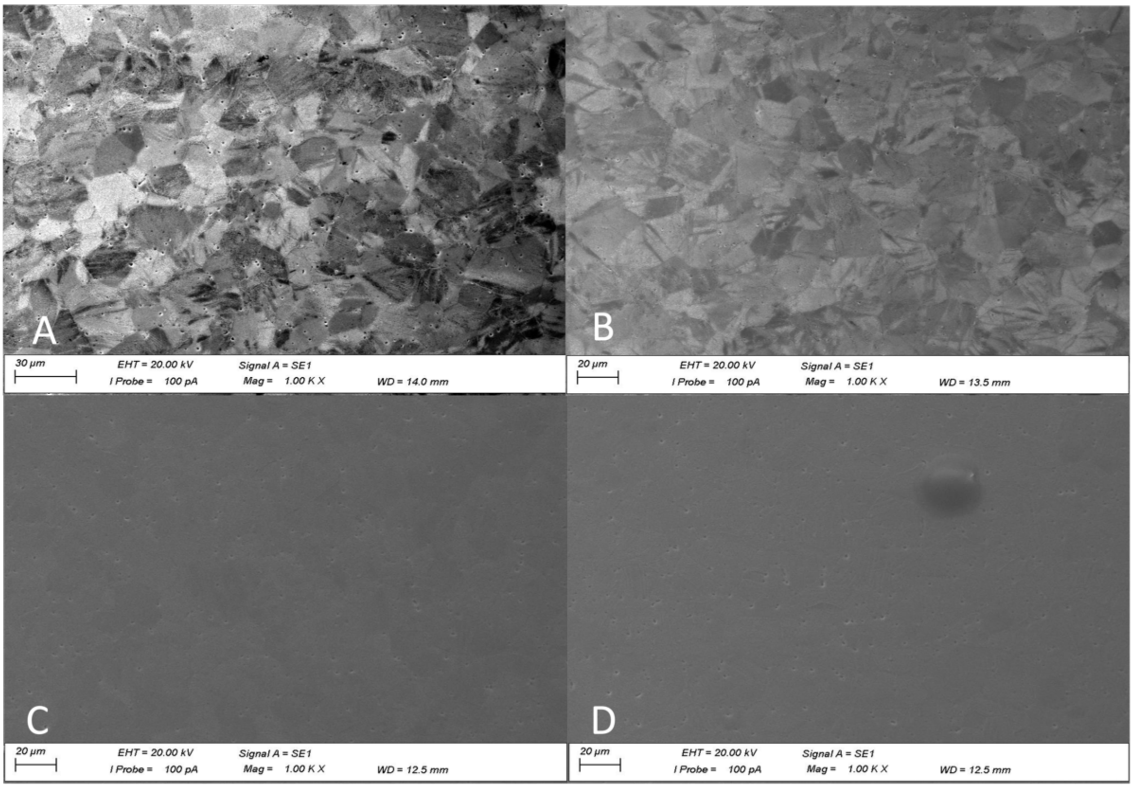

Figure 5. In electron microscopy images, both concentrated nitric acid (A) and diluted nitric acid (B) resulted in an anisotropic surface. In the case of concentrated phosphoric acid (C), the crystal boundaries were barely detectable, while the use of diluted phosphoric acid (D) exhibited a relatively homogeneous surface. (source: personal)

Lower contact angle values were expected on the surfaces with visible borders. However, the treatment of the NP samples with ccH_3PO_4 significantly reduced ($p = 0.00$) the contact angle compared to the untreated control or, in other words, increased the wettability of the NP surface (Figure 6). The coefficient of variance was less than 14%, meaning that the samples were either homogenous or low heterogenous; therefore, the wettability of the samples could be described using the mean of the measured values of the contact angle (Table 6). [100]

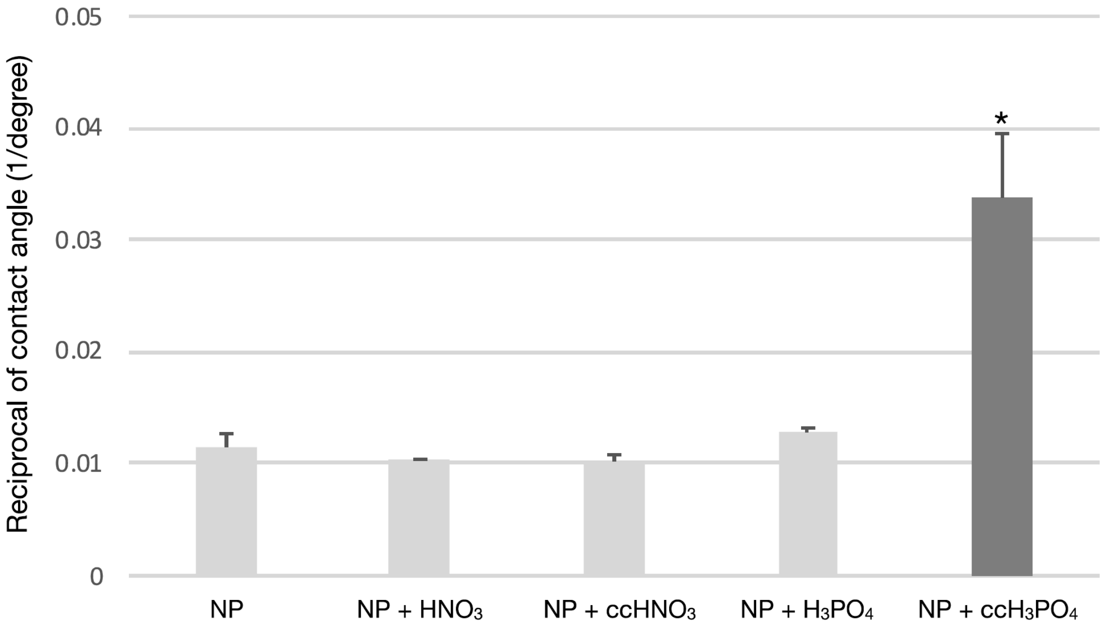

Figure 6. The effect of surface treatments on the wettability of NP surface. The treatment of the NP surface using ccH_3PO_4 has significantly increased the wettability compared to the untreated control (p * = 0.00). [100]

Table 6. Results of contact angle measurement. The ccH_3PO_4 treatment of NP surface significantly reduced the contact angle (p * = 0.00). The reciprocal of the mean and standard deviation (SD) values concerning contact angle were calculated for a better visualization of the results in Figure 6. [100]

Treatments	**Contact Angle (°)**			**Reciprocal of Contact Angle (1/Degree)**	
	Mean	**SD**	**CV**	**Mean**	**SD**
tgeNP	88.0	9.3	10.6	0.0115	0.0012
NP + HNO_3	97.0	1.4	1.4	0.0103	0.0001
NP + ccHNO_3	99.0	6.1	6.2	0.0102	0.0006
NP + H_3PO_4	78.0	2.5	3.2	0.0128	0.0004
NP + ccH_3PO_4	30.0 *	4.1	13.7	0.0338	0.0057

From this point forward, only the untreated control NP and the ccH_3PO_4-treated NP samples were subjected to further experiments, according to our findings with SEM and CA data. The AFM measurement confirmed the results of the optical profilometry, i.e., the surface roughness of the NP samples remained unchanged after ccH_3PO_4 treatment (Table 7 and Figure 7). [100]

Table 7. Surface roughness measured using AFM. Three regions of interest (ROI) were randomly selected on the untreated control and two on the ccH_3PO_4-treated NP surface for analysis. The treatment of NP surface with ccH_3PO_4 did not affect the surface roughness apparently. [100]

Treatments	**Surface Roughness**	
	Ra (nm)	**Rq (nm)**
NP (ROI 1)	36	45
NP (ROI 2)	43.4	61.1
NP (ROI 3)	37.6	46.7
NP + ccH_3PO_4 (ROI 1)	45.7	71.8
NP + ccH_3PO_4 (ROI 2)	39.1	49.3

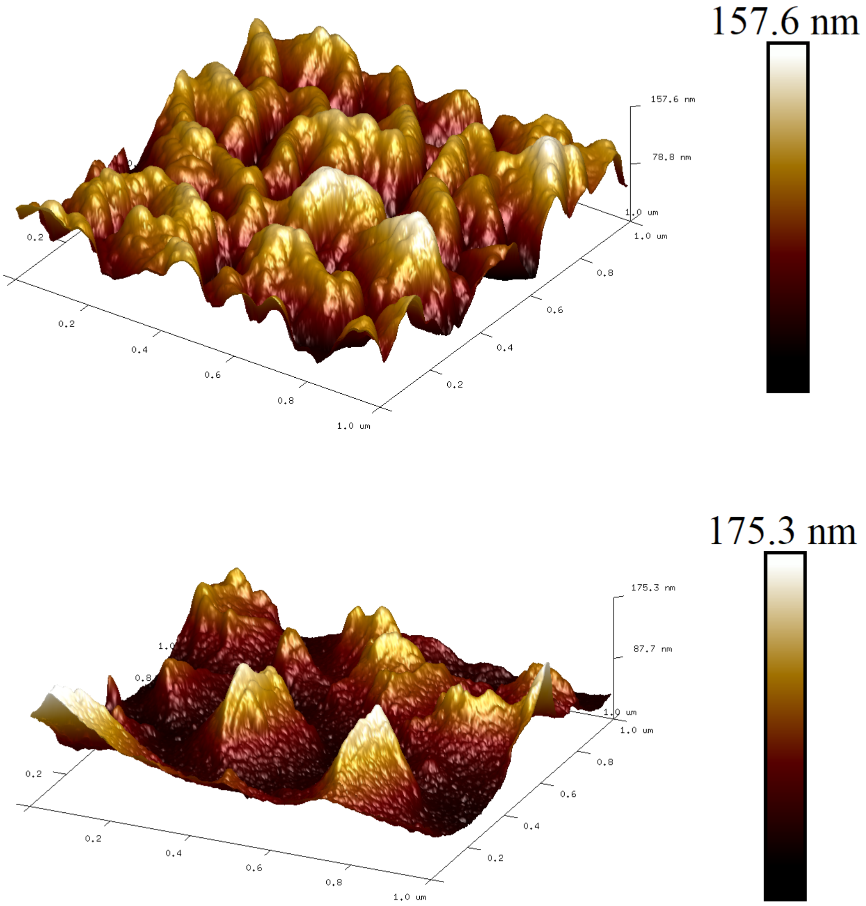

Figure 7. AFM three-dimensional (3D) image of ROI 2 of NP (left) and ROI 1 of NP+ccH_3PO_4 (right). [100]

Analyzing the surface element composition revealed approximately ten times more phosphorus on the ccH_3PO_4-treated sample (before sputtering: 7.5%; after sputtering 9.1%) compared to the untreated control NP surface (before sputtering: 0.6%; after sputtering: 0.9%) (Table 8). The proportion of O to Ti was 7.4 on the ccH_3PO_4-treated sample before sputtering and it dropped to 3.8 after sputtering. The proportion of O to Ti was 10.3 on the untreated control NP sample before sputtering and it dropped to 3.1 after sputtering. Interestingly, 41.5% less carbon appeared on the surface of the ccH_3PO_4-treated NP surface than on the untreated control (Figure 8). [100]

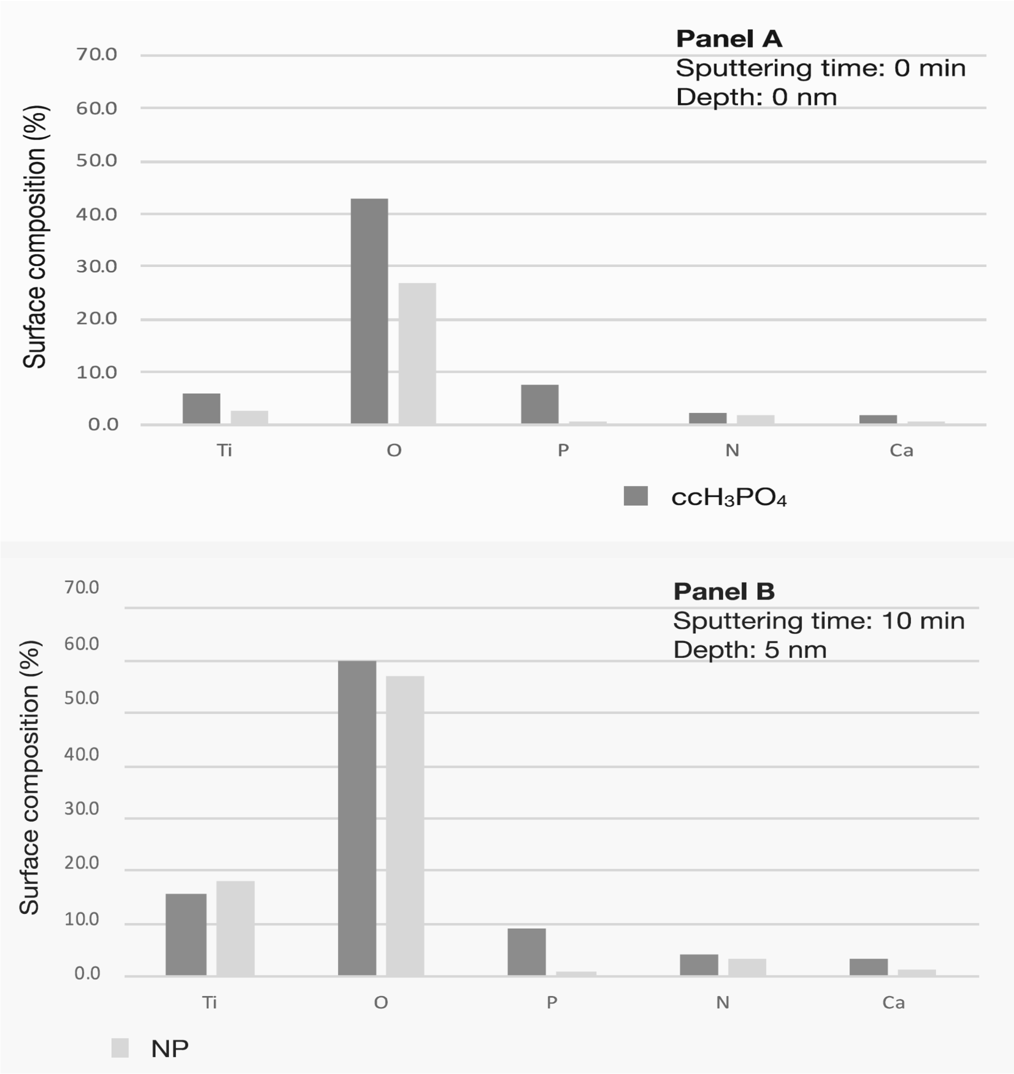

Figure 8. Proportion of elements on the untreated control and the ccH_3PO_4-treated NP surfaces. Panel A shows that the concentrations of phosphorus and oxygen are higher on the ccH_3PO_4-treated NP surface than on the untreated control. Panel B shows that the proportion of phosphorus did not change on the control or on the ccH_3PO_4-treated NP surfaces after sputtering. Carbon concentration is intentionally omitted because it would have caused the visualization of the other elements to be difficult (see Table 3 for data). [100]

Table 8. Element composition of untreated control and ccH$_3$PO$_4$-treated NP surfaces. Ten times more phosphorus was detected on the ccH$_3$PO$_4$-treated NP surface than on the control before and after sputtering. Approximately three times more calcium appeared on the ccH$_3$PO$_4$-treated NP surface than on the untreated control even after sputtering. Carbon and nitrogen measurements were presumably contaminations from the ambient air. [100]

Sample Name	Sputtering [min]	Depth [nm]	C	Ti	O	P	N	Ca
NP + ccH$_3$PO$_4$	0	0	38.7	5.8	43.0	7.5	2.4	2.0
NP + ccH$_3$PO$_4$	10	5	6.0	15.7	60.0	9.1	4.2	3.5
NP	0	0	66.1	2.6	26.9	0.6	1.9	0.5
NP	10	5	18.9	18.3	56.9	0.9	3.5	1.5

The XPS spectrum of the untreated control NP surface showed that the Ti 2$p_{3/2}$ peak appeared at 459.1 eV binding energy indicating fully oxidized titanium (Ti^{4+}) in the TiO$_2$ oxide layer. When analyzing the ccH$_3$PO$_4$-treated NP surface, an additional peak appeared on the spectrum at 458.8 eV binding energy beside the peak at 459.7 eV, thus indicating the presence of less oxidized titanium (Ti^{3+}) beside the Ti^{4+} in the TiO$_2$ layer (Figure 9) [100, 102].

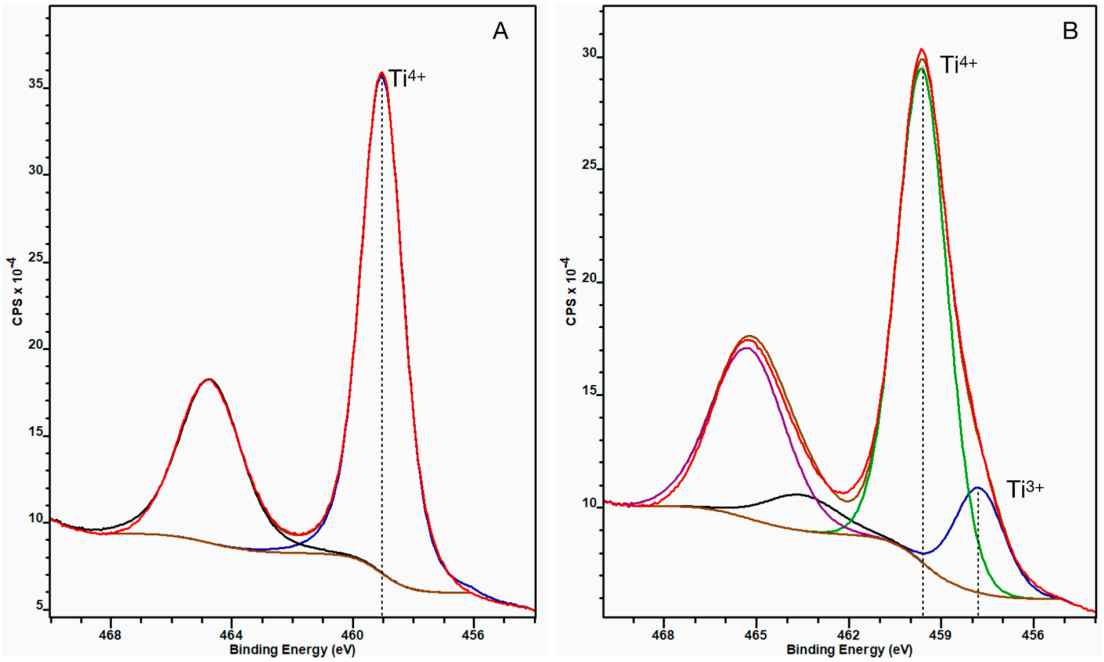

Figure 9. XPS spectra of untreated control (A) and ccH$_3$PO$_4$-treated NP surfaces (B) after sputtering. The Ti 2$p_{3/2}$ peak appeared at 459.1 eV (blue curve) for the untreated NP surface, indicating fully coordinated Ti^{4+} ions, suggesting the oxide layer was solely constituted of TiO$_2$. (The black curve is the corresponding Ti 2$p_{1/2}$ component of the doublet peak.) On panel B, an additional doublet peak appeared at 458.8 eV binding energy, which indicates the presence of Ti^{3+} beside Ti^{4+} in the oxide layer. (Here the blue curve is Ti^{3+} 2$p_{3/2}$, the green one is Ti^{4+} 2$p_{3/2}$, while the black and purple curves are the corresponding Ti^{3+}2p_1/2 and Ti^{4+} 2$p_{1/2}$ components of the doublets). [100]

5. DISCUSSION

5.1. Experimental group setup

The relatively simple microstructure and excellent biocompatibility of commercially pure titanium, combined with the less aggressive etchants, were expected to achieve a uniform effect. Commercially pure titanium has a single-phase alpha structure, while alloys (like Grade 5) consist of biphasic crystals (alpha and beta). This complex microstructure means that Grade 5 titanium does not etch as uniformly as Grade 2, and the presence of the beta phase increases its overall resistance to acid attacks. [103, 104] Recently, concerns have been raised on the potential toxicity of a few, specific alloys, such as titanium Grade 5 or Nitinol, due to the presence of aluminum/vanadium and nickel, respectively. [82] Strong acids like hydrochloric acid (HCl) and sulfuric acid (H_2SO_4), along with prolonged etching durations, can lead to the formation of titanium hydride (TiH_2), which increases the brittleness of the surface layer. These brittle hydride phases can result in ion leaching, which may cause short-term pain and inflammation, and contribute to bone loss over time, as supported by the literature [103] *Park et al.* reported that phosphoric acid treatment on titanium surfaces enhances osteoblast attachment, differentiation, and biomechanical anchorage by creating micro-rough, hydrophilic, and phosphorus-incorporated oxide layers. Their study demonstrated that phosphoric acid can significantly improve surface wettability, induce better cell responses and stronger bone-implant integration, as evidenced by increased removal torque forces in rabbit tibiae. [105] These findings suggest that phosphoric acid treatment could be an effective method for optimizing titanium implants for better osseointegration. Based on the findings from *Prando et al.*, titanium exhibits superior corrosion resistance in phosphoric acid (H_3PO_4) and nitric acid compared to hydrochloric acid (HCl) and sulfuric acid (H_2SO_4). This resistance is reflected in significantly lower corrosion rates, indicating that phosphoric acid and nitric acid is less aggressive towards the TiO_2 layer. [106]

5.2 Null Hypotheses

Null Hypothesis 1 ($H0_1$)

The applied etchants and parameters do not induce any changes in the properties of nano-pitted titanium oxide surfaces.

Acid etching is most commonly performed after a sandblasting step to remove blasting residues and to refine the surface morphology and roughness. [107] Studies usually report the use of more agressive etchants, such as H_2SO_4 or HCl for 10 minutes of etching duration above room temperature to reach the desired topographical changes. [103, 108] Hydrothermal treatment with dilute H_3PO_4 has also been investigated on 180 °C. [105] According to the literature we hypothesized that our etching parameters will not lead to any changes to the NP surface. The results from the SEM revealed grain boundaries, which suggests that our etching process effectively exposed the microstructural features of the discs, potentially impacting its mechanical properties, corrosion behavior, and overall surface reactivity. This observation indicates that the etching process did indeed alter the surface properties of the nano-pitted titanium oxide, leading us to reject $H0_1$ and conclude that the applied etchants and parameters did induce changes in the properties of nano-pitted titanium oxide surfaces.

Null Hypothesis 2 ($H0_2$)

The applied etchants and parameters result in similar surface roughness on the nano-pitted structure.

The optical profilometry results showed no significant differences in surface roughness between the experimental groups and the untreated NP control, leading us to fail to reject $H0_2$ and conclude that etching did not alter the surface roughness of the NP samples. The rejection of $H0_1$ and the failure to reject $H0_2$ indicate that while the different etchants modified the NP surface, the surface topography remained unchanged. The investigation of AFM on both concentrated H_3PO_4-treated discs and untreated NP discs revealed no significant difference in nano-level roughness. The presence of both concentrated and dilute acids in the experimental groups indicates the good resistance of the NP topography to chemical exposure. These findings reinforce the chemical resilience of the NP surface, aligning with the earlier report of *Weszl et al.* that NP anodic surfaces yield significantly better mechanical resistance compared to the widely investigated nanotubular anodic films [84] The mechanical and chemical resistance causes the treatment of NP films with ccH_3PO_4 to be a promising candidate among the surface treatment of titanium. The resistance to chemical exposure is relevant because it allows the functionalization of the NP surface either with chemical or biological compounds to enhance the bioactivity of implants. Since the antibacterial effect of the NP surface is related to the texture distribution of its nanostructure [85, 87, 109], we can assume that it retains a good portion of this property after the treatment. [100]

Null Hypothesis 3 ($H0_3$)

The applied etchants and parameters do not induce significant changes in the hydrophilicity of the nano-pitted titanium oxide surface.

It was surprising to observe how significantly a simple etching of the NP surface with concentrated phosphoric acid increased its hydrophilicity. The results showed that the concentrated phosphoric acid treatment significantly enhanced the hydrophilicity of the NP surface, while dilute phosphoric acid and nitric acid had minimal impact. [100] Consequently, $H0_3$ was rejected.

Summary of Null Hypotheses

The rejection of both $H0_1$ and $H0_3$ indicates that the etching process notably altered the surface properties and significantly increased hydrophilicity of the NP samples when using ccH_3PO4. However, $H0_2$ was not rejected, as no significant changes in surface roughness were observed. These results suggest that while the etching process with ccH_3PO_4 exposes underlying microstructural features and increases hydrophilicity, the nano-pitted topography itself remains unaffected. The treatment with ccH_3PO_4 resulted in a presumably larger, homogenous surface. The AFM measurements align with documented effects of acid etching, where the surface area increases without significantly altering the average height deviation. (Figure 7) Additionally, they confirm that the etching process converts surface anisotropy into isotropy. [110] Etching may offer a simple and adaptable method to modify the wettability of TiO_2 surfaces. [111] Recently, phosphoric acid has raised a great deal of interest because of its ability to improve the bioactivity of titanium implants. The phosphorus functionalization of TiO_2 surfaces has been proven to be a potent approach to enhance both the catalytic and the biological properties of titanium. [105, 112] However, the current methods of phosphorus-functionalization often apply concomitant exposure of phosphoric acid and physical energy (such as thermal or electrochemical treatment) to the TiO_2 surface, which may irreversibly change the surface morphology. [100, 113]

5.3 Hydrophilicity

The appearance of the surface charge might be responsible for the raise in hydrophilicity of the NP surface after phosphoric acid treatment. There are two possible underlying mechanisms: (i) the presence of surface charges that can facilitate the adsorption of more water molecules than onto uncharged the TiO_2 surface and (ii) the surface charge seemingly prevented the adhesion of hydrocarbons from the ambient air that were known to be responsible for the deterioration of the hydrophilicity of the TiO_2 surfaces. [100] These mechanisms were investigated using XPS, which provided insights into the surface chemistry and elemental composition. The concentrated phosphoric acid was assumed strong enough to penetrate the uppermost layer of TiO_2 where the phosphate ions chemically reacted with the titanium. Based on the available data, it is not possible to explain the entire reaction mechanism, however the appearance of the $2p_{3/2}$ peak at 458.8 eV binding energy on the XPS spectra of the concentrated phosphoric acid-treated NP surface suggests that a redox reaction occurred on the surface. The only known explanation of the asymmetric peak broadening of the XPS peak (Figure 9) is the presence of another chemical state, which corresponds to Ti^{3+} suggesting that the concentrated phosphoric acid treatment caused the decrease in the oxidation state of titanium ($Ti4^{+} \rightarrow Ti3^{+}$) in the oxide layer. The proportion of absorbed phosphorus significantly increased after concentrated phosphoric acid treatment of the NP surface compared to the untreated control. [100] *Connor and McQuillan*'s study demonstrates that phosphate ions strongly bind to TiO2 surfaces, forming stable bidentate species. This suggests that phosphorus adsorption has an impact on surface properties, but may require further refinement to fully explain the specific physicochemical changes observed in our findings, particularly regarding hydrophilicity and surface reactivity. [100, 114]. The oxidation state of the adhered phosphorus is not known. Interestingly, the proportion of carbon was more than 40% less on the phosphoric acid-treated NP surface than on the control. However, the presence of three times more calcium on the surface of the concentrated phosphoric acid-treated NP surface suggests that the phosphorus is coordinated with oxygen (O^-) that can bind cations, such as calcium. Given that calcium is ubiquitous in the human body, in blood and interstitial fluids, the implant surface is exposed to it after surgical insertion. The coordination of phosphorous with calcium ions might increase the quantity and volume of charges on the titanium surface [100, 115]. The increase in calcium and phosphorus suggests the enhancement of the biological and catalytic properties of the titanium surface [100, 105, 112, 116, 117], which is further improved by the appearance of Ti^{3+} oxidation state. While Ti^{4+} is chemically stable, it is also underlined in the literature that the success of some materials, often depends on their chemical activity. [32]

Observation of extended hydrophilicity

Recently wettability gained increased attention. [118, 119] Various techniques have been suggested to increase hydrophilicity of titanium oxide surfaces. [52] One such widely anticipated method is sandblasting and double etching followed by drying under nitrogen protection to prevent exposure to air and then storing implants in a sealed glass tube containing isotonic NaCl solution. However, whith the dissipation of NaCl the superhydrophilicity feature diminishes. [120] Other studies have been published touting the benefits of UV irradiation that temporary turned dental implant surfaces to super hydrophilic, albeit they returned to a hydrophobic state in the dark. [121] *Ueno et al.* argues in favor of gamma-irradiation to regain the hydrophilicity and bioactivity of titanium implants that are lost over time owing to hydrocarbon deposition from the atmosphere [122]. However, a 25–35 kGy dose of gamma irradiation, which is generally used for the sterilization of titanium implants, might cause irreversible alteration to the TiO_2 nanosurfaces as has been the case in other nanoparticles of various materials [123, 124]. Thermal treatment can also temporarily increase the hydrophilicity of titanium implants, but the effect often decreases over time, and the heat may modify the surface morphology [125, 126]. *Lee JH et al.* argues that the degree of hydrophilicity would be a determinant for the bioactivity level of titanium surfaces. [127] They highlight a time-dependent alteration in the physicochemical properties of titanium, referred to as the biological aging of titanium, which impacts its biological capabilities. A notable change during this process is the disappearance of hydrophilic nature. However, their study was limited to a 4-week period and specifically focused on the superhydrophilic nature of sandblasted and double-etched surfaces. During this time, the contact angle increased from 5 degrees to over 60 degrees, and the carbon content rose from 14% to 63%. [127] The study also highlights the impact of hydrocarbon accumulation on wettability behavior, emphasizing the significant decline in hydrophilic properties on these types of surfaces. As an extension of our study we measured the hydrophilicity of NP discs treated with concentrated orthophosphoric acid after 6 months of preparation. (Figure 10) The discs were stored in sealed containers without any storage medium. The contact angle increased from 30 degrees to 63 degrees, which is still considered to be in the hydrophilic range (0-90 degrees). Refering to *Lee JH et al.* the NP discs also showed the sign of aging of titanium but unlike the superhydrophilic surfaces they examined, which rapidly lost their hydrophilicity, the phosphoric acid-treated surfaces maintained a level of hydrophilicity significantly longer.

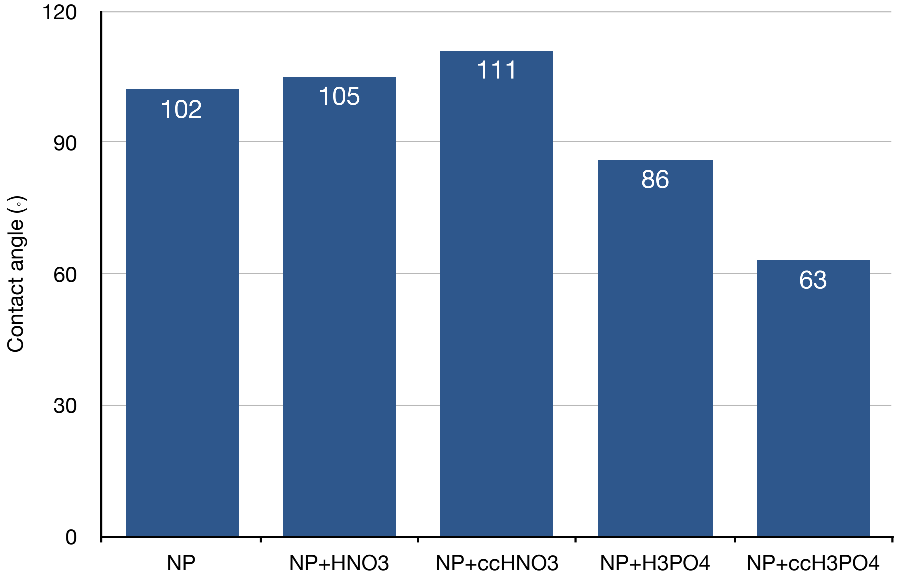

Figure 10. Contact angle measurements after 6 months of preparation still highlight notable hydrophilicity on the ccH_3PO_4 treated NP titanium oxide surface.

5.4. Limitations of the study

The results of this study should be interpreted with consideration of its limitations. Factors such as the geometry of dental implants may affect the uniformity of phosphoric acid treatment across the surface, raising questions about the adaptability of the applied surface-treatment method. Additionally, in industrial-scale manufacturing, precise control of treatment parameters, particularly temperature, is crucial to ensure the uniformity of the final products. These challenges could not be fully addressed in laboratory-scale experiments. Furthermore, the corrosion and mechanical resistance of the NP TiO_2 surface treated with concentrated H_3PO_4 require further investigation before conclusions can be made regarding the industrial applicability of this surface-treatment method. [100]

5.1. New findings

Based on the literature, it can be hypothetized that nanoscale surface modifications may involve quantum effects, which should be examined through an interdisciplinary approach in implant surface modification procedures.

In our study, we highlight the following as novel findings:

1. The hydrophilicity of the nano-pitted surface on Grade 2 titanium discs is significantly increased by etching with concentrated phosphoric acid (85%)

2. The hydrophilicity of the nano-pitted surface on Grade 2 titanium discs is maintained long-term as a result of etching with concentrated phosphoric acid (85%)

3. We were the first to describe in the international literature the modification of the nano-pitted surface with concentrated phosphoric acid, which resulted in a durable hydrophilic surface even when stored in a liquid-free environment.

6. CONCLUSIONS

The main goal of our study was to increase the hydrophilic property on a surface with nanotopographical features through acid etching while preserving its structural characteristics. We reproduced the nano-pitted [84] titanium oxide surface and investigated the effect of various etchants on it. Surface characterization techniques such as SEM, contact angle measurement, AFM, and XPS were performed to evaluate the morphological and chemical changes induced by the etching processes. The results demonstrated that the use of concentrated phosphoric acid significantly increased the hydrophilicity of the nano-pitted surface without affecting the uniformity or the integrity of the surface. Additionally, we found that other etchants, including dilute phosphoric acid, dilute nitric acid and even concentrated nitric acid had minimal impact on hydrophilicity and did not induce significant changes in surface roughness. Besides the significant changes in wettability our study also demonstrated the reproducability and potential corrosion resistance of the nano-pitted titanium oxide surface. The XPS analysis revealed that the concentrated phosphoric acid treatment led to an increase in surface phosphorus content, indicating successful chemical modification of the nano-pitted titanium oxide surface. Additionally, there was a notable reduction in surface hydrocarbons, which is likely attributed to the enhanced surface cleaning effect of the acid etching. In conclusion, the etching of the nano-pitted TiO_2 surface with ccH_3PO_4 improved its wettability and did not destroy the nano-topography. [100] Our study shows unique combination of anodization and acid etching that might be subject to further investigations. The homogeneous nanostructured titanium surface, in combination with acid etching, is expected to lead to uniform material properties, ensuring consistent surface behavior during subsequent treatments and preserving the integrity and performance of the titanium under various conditions. This approach is grounded in scientifically and clinically established methods aimed at ensuring biocompatibility and potential bioactivity while minimizing redundant processing effects.

7. SUMMARY

In dental implantology, titanium plays a crucial role due to its material properties. Its biocompatibility is attributed to the spontaneously formed TiO_2 layer on its surface. Various surface treatment procedures have shown that increasing surface roughness positively impacts the integration of implants. Clinical experience, material science knowledge, and technological advancements have also made it clear that, in addition to surface roughness and chemical composition, other properties significantly influence osseointegration. These include the wettability and antibacterial effect of titanium surfaces, which represent one of the main challenges in the nanoscale modifications of titanium surfaces. However, the transferability of scientific achievements from experimental settings to industrial-scale manufacturing is often limited by the low productivity of the underlying technologies. Nano-pitted anodic films have already demonstrated significant effects on osseointegration, antibacterial properties, mechanical resistance, and high reproducibility. [100] Our study showed that concentrated orthophosphoric acid significantly enhances the hydrophilicity of such surfaces without disrupting the nano-topography. Furthermore, this hydrophilicity is maintained over the long term without requiring special storage conditions. There is no documented surface treatment method in the literature that ensures the long-term preservation of the hydrophilicity of nanomorphological titanium oxide surfaces. Additionally, we assume that the nano-pitted surface treated with concentrated othophosphoric acid retains a good portion the related antibacterial effect, since it is related to the texture distribution of its nanostructure. This assumption can be further explored and validated in future studies. Our findings thus represent a potential breakthrough in surface treatment techniques for titanium implants, combining presumably enhanced biological properties with the practicality of industrial-scale application.

8. REFERENCES

1. Fürst MM, Salvi GE, Lang NP, Persson GR. Bacterial colonization immediately after installation on oral titanium implants. Clin Oral Implants Res. 2007;18(4):501-8. doi:10.1111/j.1600-0501.2007.01381.x.

2. Dhir S. Biofilm and dental implant: The microbial link. J Indian Soc Periodontol. 2013;17(1):5-11. doi:10.4103/0972-124X.107466.

3. Gristina AG. Biomaterial-centered infection: microbial adhesion versus tissue integration. Science. 1987;237(4822):1588-95. doi:10.1126/science.3629258.

4. Marin E, Boschetto F, Pezzotti G. Biomaterials and biocompatibility: An historical overview. J Biomed Mater Res A. 2020;108(8):1617-33. doi:10.1002/jbm.a.36930.

5. Branemark P-I. Osseointegration and its experimental background. J Prosthet Dent. 1983;50(3):399-410. doi:10.1016/S0022-3913(83)80101-2.

6. Williams DF, editor Definitions in biomaterials : proceedings of a consensus conference of the European Society for Biomaterials, Chester, England, March 3-5, 1986.

7. . Introduction. In: Williams D, Zhang X, editor(s). Definitions of Biomaterials for the Twenty-First Century. Amsterdam: Elsevier; 2019. pp. 1-14.

8. . Biomaterials and biomedical materials. In: Williams D, Zhang X, editor(s). Definitions of Biomaterials for the Twenty-First Century. Amsterdam: Elsevier; 2019. pp. 15-23.

9. Rupp F, Geis-Gerstorfer J, Geckeler KE. Dental implant materials: Surface modification and interface phenomena. Adv Mater. 1996;8(3):254-7. doi:10.1002/adma.19960080316.

10. Budei DV, Vaireanu DI, Prepelita P, Popescu-Pelin G, Mincu M, Ciobotaru IA. A comparative morphological study of titanium dioxide surface layer dental implants. Open Chem. 2021;19(1):189-98. doi:10.1515/chem-2021-0197.

11. Weeks ME. The discovery of the elements. XI. Some elements isolated with the aid of potassium and sodium: Zirconium, titanium, cerium, and thorium. J Chem Educ. 1932;9(7):1231. doi:10.1021/ed009p1231.

12. Brånemark PI, Adell R, Albrektsson T, Lekholm U, Lundkvist S, Rockler B. Osseointegrated titanium fixtures in the treatment of edentulousness. Biomaterials. 1983;4(1):25-8. doi:10.1016/0142-9612(83)90065-0.

13. Brånemark PI, Breine U, Adell R, Hansson BO, Lindström J, Ohlsson Å. Intra-Osseous Anchorage of Dental Prostheses: I. Experimental Studies. Scand J Plast Reconstr Surg. 1969;3(2):81-100. doi:10.3109/02844316909036699.

14. Meirelles L. On nano size structures for enhanced early bone formation [dissertation]. Gothenburg: University of Gothenburg; 2007.

15. Ericsson I, Randow K, Glantz PO, Lindhe J, Nilner K. Clinical and radiographical features of submerged and nonsubmerged titanium implants. Clin Oral Implants Res. 1994;5(3):185-9. doi:10.1034/j.1600-0501.1994.050310.x.

16. Buser D, Weber HP, Lang NP. Tissue integration of non-submerged implants. 1-year results of a prospective study with 100 ITI hollow-cylinder and hollow-screw implants. Clin Oral Implants Res. 1990;1(1):33-40. doi:10.1034/j.1600-0501.1990.010105.x.

17. Block MS, Kent JN, Kay JF. Evaluation of hydroxylapatite-coated titanium dental implants in dogs. J Oral Maxillofac Surg. 1987;45(7):601-7. doi:10.1016/0278-2391(87)90270-9.

18. Czumbel LM, Kerémi B, Gede N, Mikó A, Tóth B, Csupor D, Szabó A, Farkasdi S, Gerber G, Balaskó M, Pétervári E, Sepp R, Hegyi P, Varga G. Sandblasting reduces dental implant failure rate but not marginal bone level loss: A systematic review and meta-analysis. PLoS One. 2019;14(5):e0216428. doi:10.1371/journal.pone.0216428.

19. Esposito M, Hirsch JM, Lekholm U, Thomsen P. Biological factors contributing to failures of osseointegrated oral implants. (II). Etiopathogenesis. Eur J Oral Sci. 1998;106(3):721-64. doi:10.1046/j.0909-8836..t01-6-.x.

20. Esposito M, Hirsch JM, Lekholm U, Thomsen P. Failure patterns of four osseointegrated oral implant systems. J Mater Sci Mater Med. 1997;8(12):843-7. doi:10.1023/a:1018593403126.

21. Wennerberg A, Albrektsson T. Suggested guidelines for the topographic evaluation of implant surfaces. Int J Oral Maxillofac Implants. 2000;15(3):331-44.

22. Wennerberg A, Hallgren C, Johansson C, Danelli S. A histomorphometric evaluation of screw-shaped implants each prepared with two surface roughnesses. Clin Oral Implants Res. 1998;9(1):11-9. doi:10.1034/j.1600-0501.1998.090102.x.

23. Junker R, Dimakis A, Thoneick M, Jansen JA. Effects of implant surface coatings and composition on bone integration: a systematic review. Clin Oral Implants Res. 2009;20:185-206. doi:10.1111/j.1600-0501.2009.01777.x.

24. Buser D, Schenk RK, Steinemann S, Fiorellini JP, Fox CH, Stich H. Influence of surface characteristics on bone integration of titanium implants. A histomorphometric study in miniature pigs. J Biomed Mater Res. 1991;25(7):889-902. doi:10.1002/jbm.820250708.

25. Roccuzzo A, Imber JC, Marruganti C, Salvi GE, Ramieri G, Roccuzzo M. Clinical outcomes of dental implants in patients with and without history of periodontitis: A 20-

year prospective study. J Clin Periodontol. 2022;49(12):1346-56. doi:10.1111/jcpe.13716.

26. Kwon T, Bain PA, Levin L. Systematic review of short- (5-10 years) and long-term (10 years or more) survival and success of full-arch fixed dental hybrid prostheses and supporting implants. J Dent. 2014;42(10):1228-41. doi:10.1016/j.jdent.2014.05.016.

27. Buser D, Janner SF, Wittneben JG, Brägger U, Ramseier CA, Salvi GE. 10-year survival and success rates of 511 titanium implants with a sandblasted and acid-etched surface: a retrospective study in 303 partially edentulous patients. Clin Implant Dent Relat Res. 2012;14(6):839-51. doi:10.1111/j.1708-8208.2012.00456.x.

28. Lang NP, Salvi GE, Huynh-Ba G, Ivanovski S, Donos N, Bosshardt DD. Early osseointegration to hydrophilic and hydrophobic implant surfaces in humans. Clin Oral Implants Res. 2011;22(4):349-56. doi:10.1111/j.1600-0501.2011.02172.x.

29. Thakral GK, Thakral R, Sharma N, Seth J, Vashisht P. Nanosurface - The Future of Implants. J Clin Diagn Res. 2014;8(5):ZE7-ZE10. doi:10.7860/jcdr/2014/8764.4355.

30. Bauer S, Schmuki P, von der Mark K, Park J. Engineering biocompatible implant surfaces: Part I: Materials and surfaces. Prog Mater Sci. 2013;58(3):261-326. doi:10.1016/j.pmatsci.2012.09.001.

31. Kasemo B, Lausmaa J. Material-tissue interfaces: the role of surface properties and processes. Environ Health Perspect. 1994;102 Suppl 5:41-5. doi:10.1289/ehp.94102s541.

32. Schwartz Z, Boyan BD. Underlying mechanisms at the bone-biomaterial interface. J Cell Biochem. 1994;56(3):340-7. doi:10.1002/jcb.240560310.

33. Nanci A, Wuest JD, Peru L, Brunet P, Sharma V, Zalzal S, McKee MD. Chemical modification of titanium surfaces for covalent attachment of biological molecules. J Biomed Mater Res. 1998;40(2):324-35. doi:10.1002/(sici)1097-4636(199805)40:2<324::aid-jbm18>3.0.co;2-l.

34. Cooper LF. Biologic determinants of bone formation for osseointegration: clues for future clinical improvements. J Prosthet Dent. 1998;80(4):439-49. doi:10.1016/s0022-3913(98)70009-5.

35. Schwartz Z, Lohmann CH, Oefinger J, Bonewald LF, Dean DD, Boyan BD. Implant surface characteristics modulate differentiation behavior of cells in the osteoblastic lineage. Adv Dent Res. 1999;13:38-48. doi:10.1177/08959374990130011301.

36. Ehrenfest DMD, Coelho PG, Kang BS, Sul YT, Albrektsson T. Classification of osseointegrated implant surfaces: materials, chemistry and topography. Trends Biotechnol. 2010;28(4):198-206. doi:10.1016/j.tibtech.2009.12.003.

37. Hotchkiss KM, Reddy GB, Hyzy SL, Schwartz Z, Boyan BD, Olivares-Navarrete R. Titanium surface characteristics, including topography and wettability, alter macrophage activation. Acta Biomater. 2016;31:425-34. doi:10.1016/j.actbio.2015.12.003.

38. Hotchkiss KM, Clark NM, Olivares-Navarrete R. Macrophage response to hydrophilic biomaterials regulates MSC recruitment and T-helper cell populations. Biomaterials. 2018;182:202-15. doi:10.1016/j.biomaterials.2018.08.029.

39. Abaricia JO, Shah AH, Chaubal M, Hotchkiss KM, Olivares-Navarrete R. Wnt signaling modulates macrophage polarization and is regulated by biomaterial surface properties. Biomaterials. 2020;243. doi:10.1016/j.biomaterials.2020.119920.

40. Webster TJ, Ergun C, Doremus RH, Siegel RW, Bizios R. Enhanced functions of osteoblasts on nanophase ceramics. Biomaterials. 2000;21(17):1803-10. doi:10.1016/s0142-9612(00)00075-2.

41. Tomsia AP, Lee JS, Wegst UG, Saiz E. Nanotechnology for dental implants. Int J Oral Maxillofac Implants. 2013;28(6):535-46. doi:10.11607/jomi.te34.

42. Hayashi M, Jimbo R, Lindh L, Sotres J, Sawase T, Mustafa K, Andersson M, Wennerberg A. In vitro characterization and osteoblast responses to nanostructured photocatalytic TiO2 coated surfaces. Acta Biomater. 2012;8(6):2411-6. doi:10.1016/j.actbio.2012.03.010.

43. Gittens RA, Olivares-Navarrete R, McLachlan T, Cai Y, Hyzy SL, Schneider JM, Schwartz Z, Sandhage KH, Boyan BD. Differential responses of osteoblast lineage cells to nanotopographically-modified, microroughened titanium-aluminum-vanadium alloy surfaces. Biomaterials. 2012;33(35):8986-94. doi:10.1016/j.biomaterials.2012.08.059.

44. Barberi J, Spriano S. Titanium and protein adsorption: an overview of mechanisms and effects of surface features. Materials (Basel). 2021;14(7):1590. doi:10.3390/ma14071590.

45. Zhang C, Zhang TJ, Geng TY, Wang XD, Lin KL, Wang PL. Dental implants loaded with bioactive agents promote osseointegration in osteoporosis: a review. Front Bioeng Biotechnol. 2021;9:591796. doi:10.3389/fbioe.2021.591796.

46. Xiao YC, Ding YS, Zhuang JW, Sun RY, Sun H, Bai L. Osteoimmunomodulation role of exosomes derived from immune cells on osseointegration. Front Bioeng Biotechnol. 2022;10:989537. doi:10.3389/fbioe.2022.989537.

47. Mendonça G, Mendonça DBS, Aragao FJL, Cooper LF. Advancing dental implant surface technology - From micron- to nanotopography. Biomaterials. 2008;29(28):3822-35. doi:10.1016/j.biomaterials.2008.05.012.

48. Kang MK, Moon SK, Kim KM, Kim KN. Antibacterial effect and cytocompatibility of nano-structured TiO2 film containing Cl. Dent Mater J. 2011;30(6):790-8. doi:10.4012/dmj.2011-021.

49. Souza JCM, Sordi MB, Kanazawa M, Ravindran S, Henriques B, Silva FS, Aparicio C, Cooper LF. Nano-scale modification of titanium implant surfaces to enhance osseointegration. Acta Biomater. 2019;94:112-31. doi:10.1016/j.actbio.2019.05.045.

50. Zambuzzi WF, Coelho PG, Alves GG, Granjeiro JM. Intracellular signal transduction as a factor in the development of "smart" biomaterials for bone tissue engineering. Biotechnol Bioeng. 2011;108(6):1246-50. doi:10.1002/bit.23117.

51. Kieswetter K, Schwartz Z, Dean DD, Boyan BD. The role of implant surface characteristics in the healing of bone. Crit Rev Oral Biol Med. 1996;7(4):329-45. doi:10.1177/10454411960070040301.

52. Gittens RA, Scheideler L, Rupp F, Hyzy SL, Geis-Gerstorfer J, Schwartz Z, Boyan BD. A review on the wettability of dental implant surfaces II: Biological and clinical aspects. Acta Biomater. 2014;10(7):2907-18. doi:10.1016/j.actbio.2014.03.032.

53. van Oirschot B, Zhang Y, Alghamdi HS, Cordeiro JM, Nagay BE, Barao VAR, de Avila ED, van den Beucken J. Surface engineering for dental implantology: favoring tissue responses along the implant. Tissue Eng Part A. 2022;28(11-12):555-72. doi:10.1089/ten.tea.2021.0230.

54. Bayda S, Adeel M, Tuccinardi T, Cordani M, Rizzolio F. The history of nanoscience and nanotechnology: from chemical-physical applications to nanomedicine. Molecules. 2019;25(1):112. doi:10.3390/molecules25010112.

55. Augustine Ike O, Henry Ifeanyi I, Abraham Iheanyichukwu C. Surface and quantum effects in nanosized semiconductor. Am J Nano Res Appl. 2020;8(3):35-41. doi:10.11648/j.nano.20200803.11.

56. Mansoori GA, Soelaiman TAF. Nanotechnology — an introduction for the standards community. J ASTM Int. 2005;2:1-21. doi:10.1520/JAI13110.

57. Geoffrion LD, Guisbiers G. Quantum confinement: Size on the grill! J Phys Chem Solids. 2020;140:109320. doi:10.1016/j.jpcs.2019.109320.

58. Kolahalam LA, Kasi Viswanath IV, Diwakar BS, Govindh B, Reddy V, Murthy YLN. Review on nanomaterials: Synthesis and applications. Mater Today Proc. 2019;18:2182-90. doi:10.1016/j.matpr.2019.07.371.

59. Roduner E. Size matters: why nanomaterials are different. Chem Soc Rev. 2006;35(7):583-92. doi:10.1039/b502142c.

60. Wang ZS, Wang JL, Wu RF, Wei JC. Construction of functional surfaces for dental implants to enhance osseointegration. Front Bioeng Biotechnol. 2023;11. doi:10.3389/fbioe.2023.1320307.

61. Iqbal P, Preece JA, Mendes PM. Nanotechnology: The “top-down” and “bottom-up” approaches. In: Steed JW GP, editor(s). Supramol Chem. Chichesterben: John Wiley & Sons; 2012. pp. 1-14.

62. Joudeh N, Linke D. Nanoparticle classification, physicochemical properties, characterization, and applications: a comprehensive review for biologists. J Nanobiotechnology. 2022;20(1):262. doi:10.1186/s12951-022-01477-8.

63. Silva RCS, Agrelli A, Andrade AN, Mendes-Marques CL, Arruda IRS, Santos LRL, Vasconcelos NF, Machado G. Titanium dental implants: an overview of applied nanobiotechnology to improve biocompatibility and prevent infections. Materials. 2022;15(9). doi:10.3390/ma15093150.

64. Abdulghafor MA, Mahmood MK, Tassery H, Tardivo D, Falguiere A, Lan RM. Biomimetic coatings in implant dentistry: a quick update. J Funct Biomater. 2024;15(1). doi:10.3390/jfb15010015.

65. Brammer KS, Frandsen CJ, Jin S. TiO2 nanotubes for bone regeneration. Trends Biotechnol. 2012;30(6):315-22. doi:10.1016/j.tibtech.2012.02.005.

66. Buzea C, Pacheco, II, Robbie K. Nanomaterials and nanoparticles: sources and toxicity. Biointerphases. 2007;2(4):Mr17-71. doi:10.1116/1.2815690.

67. Ikhmayies SJ. Characterization of Nanomaterials. JOM. 2014;66(1):28-9. doi:10.1007/s11837-013-0826-6.

68. Abaszadeh F, Ashoub MH, Khajouie G, Amiri M. Nanotechnology development in surgical applications: recent trends and developments. Eur J Med Res. 2023;28(1):537. doi:10.1186/s40001-023-01429-4.

69. Alamoudi A. Nanoengineering and surface modifications of dental implants. Cureus. 2024;16(1). doi:10.7759/cureus.51526.

70. Wennerberg A, Galli S, Albrektsson T. Current knowledge about the hydrophilic and nanostructured SLActive surface. Clin Cosmet Investig Dent. 2011;3:59-67. doi:10.2147/cciden.S15949.

71. Shah FA, Nilson B, Brånemark R, Thomsen P, Palmquist A. The bone-implant interface - nanoscale analysis of clinically retrieved dental implants. Nanomedicine. 2014;10(8):1729-37. doi:10.1016/j.nano.2014.05.015.

72. Hasegawa M, Saruta J, Hirota M, Taniyama T, Sugita Y, Kubo K, Ishijima M, Ikeda T, Maeda H, Ogawa T. A newly created meso-, micro-, and nano-scale rough titanium surface promotes bone-implant integration. Int J Mol Sci. 2020;21(3). doi:10.3390/ijms21030783.

73. Dohan Ehrenfest DM, Vazquez L, Park YJ, Sammartino G, Bernard JP. Identification card and codification of the chemical and morphological characteristics of 14 dental implant surfaces. J Oral Implantol. 2011;37(5):525-42. doi:10.1563/aaid-joi-d-11-00080.

74. Dhatrak P, Shirsat U, Deshmukh V. Fatigue life prediction of commercial dental implants based on biomechanical parameters: a review. Mater Sci Surf Eng. 2015;3(2):221-6.

75. Gil J, Manero JM, Ruperez E, Velasco-Ortega E, Jiménez-Guerra A, Ortiz-García I, Monsalve-Guil L. Mineralization of Titanium Surfaces: Biomimetic Implants. Materials (Basel). 2021;14(11). doi:10.3390/ma14112879.

76. Zhang YF, Gulati K, Li Z, Di P, Liu Y. Dental implant nano-engineering: advances, limitations and future directions. Nanomaterials. 2021;11(10). doi:10.3390/nano11102489.

77. Alipal J, Lee TC, Koshy P, Abdullah HZ, Idris MI. Evolution of anodised titanium for implant applications. Heliyon. 2021;7(7):e07408. doi:10.1016/j.heliyon.2021.e07408.

78. Yao C, Webster TJ. Anodization: a promising nano-modification technique of titanium implants for orthopedic applications. J Nanosci Nanotechnol. 2006;6(9-10):2682-92. doi:10.1166/jnn.2006.447.

79. Zhang W, Zhang S, Liu H, Ren L, Wang Q, Zhang Y. Effects of surface roughening on antibacterial and osteogenic properties of Ti-Cu alloys with different Cu contents. J Mater Sci Technol. 2021;88:158-67. doi:10.1016/j.jmst.2021.01.067.

80. Smeets R, Stadlinger B, Schwarz F, Beck-Broichsitter B, Jung O, Precht C, Kloss F, Gröbe A, Heiland M, Ebker T. Impact of dental implant surface modifications on osseointegration. Biomed Res Int. 2016;2016. doi:10.1155/2016/6285620.

81. Rasouli R, Barhoum A, Uludag H. A review of nanostructured surfaces and materials for dental implants: surface coating, patterning and functionalization for improved performance. Biomater Sci. 2018;6(6):1312-38. doi:10.1039/c8bm00021b.

82. Marin E, Lanzutti A. Biomedical applications of titanium alloys: a comprehensive Review. Materials. 2024;17(1):114.

83. Koppány F, Bérczy K, Körmöczi K, Németh Z. [Changes in the "classical" factors influencing dental implant-osseointegration in recent decades]. Orv Hetil. 2019;160(37):1455-63. doi:10.1556/650.2019.31503.

84. Weszl M, Tóth KL, Kientzl I, Nagy P, Pammer D, Pelyhe L, Vrana NE, Scharnweber D, Wolf-Brandstetter C, Arpád JF, Bognár E. Investigation of the mechanical and chemical characteristics of nanotubular and nano-pitted anodic films on

grade 2 titanium dental implant materials. Mater Sci Eng C Mater Biol Appl. 2017;78:69-78. doi:10.1016/j.msec.2017.04.032.

85. Bierbaum S, Mulansky S, Bognár E, Kientzl I, Nagy P, Vrana NE, Weszl M, Boschke E, Scharnweber D, Wolf-Brandstetter C. Osteogenic nanostructured titanium surfaces with antibacterial properties under conditions that mimic the dynamic situation in the oral cavity. Biomater Sci. 2018;6(6):1390-402. doi:10.1039/c8bm00177d.

86. Mühl A, Szabó P, Krafcsik O, Aigner Z, Kopniczky J, Ákos N, Marada G, Turzó K. Comparison of surface aspects of turned and anodized titanium dental implant, or abutment material for an optimal soft tissue integration. Heliyon. 2022;8(8):e10263. doi:10.1016/j.heliyon.2022.e10263.

87. Han AF, Tsoi JKH, Rodrigues FP, Leprince JG, Palin WM. Bacterial adhesion mechanisms on dental implant surfaces and the influencing factors. Int J Adhes Adhes. 2016;69:58-71. doi:10.1016/j.ijadhadh.2016.03.022.

88. Matinlinna JP, Tsoi JK, de Vries J, Busscher HJ. Characterization of novel silane coatings on titanium implant surfaces. Clin Oral Implants Res. 2013;24(6):688-97. doi:10.1111/j.1600-0501.2012.02504.x.

89. Goldstein JI, Newbury DE, Michael JR, Ritchie NWM, Scott JHJ, Joy DC. Image Formation. In: Goldstein JI, Newbury DE, Michael JR, Ritchie NWM, Scott JHJ, Joy DC, editor(s). Scanning Electron Microscopy and X-Ray Microanalysis. New York, NY: Springer New York; 2018. pp. 93-110.

90. Okano Y. Scanning Electron Microscopy. In: The Surface Science Society J, editor(s). Compendium of surface and interface analysis. Singapore: Springer Singapore; 2018. pp. 563-9.

91. Kabayama K, Tero R. Optical Microscopy. In: The Surface Science Society J, editor(s). Compendium of surface and interface analysis. Singapore: Springer Singapore; 2018. pp. 413-7.

92. Fujii S. Atomic Force Microscope. In: The Surface Science Society J, editor(s). Compendium of surface and interface analysis. Singapore: Springer Singapore; 2018. pp. 33-7.

93. Law K-Y, Zhao H. Contact angle measurements and surface characterization techniques. In: Law K-Y, Zhao H, editor(s). Surface wetting: characterization, contact angle, and fundamentals. Cham: Springer International Publishing; 2016. pp. 7-34.

94. Castilho GAA, Martins MD, Macedo WAA. Surface characterization of titanium based dental implants. Braz J Phys. 2006;36(3B):1004-8. doi:10.1590/s0103-97332006000600055.

95. John F. Watts JW. Electron Spectroscopy. In, editor(s). An introduction to surface analysis by XPS and AES. 2019. pp. 1-18.

96. Nakamura M. X-Ray Photoelectron Spectroscopy. In: The Surface Science Society of J, editor(s). Compendium of surface and interface analysis. Singapore: Springer Singapore; 2018. pp. 833-42.

97. Altankov G, Grinnell F, Groth T. Studies on the biocompatibility of materials: fibroblast reorganization of substratum-bound fibronectin on surfaces varying in wettability. J Biomed Mater Res. 1996;30(3):385-91. doi:10.1002/(sici)1097-4636(199603)30:3<385::Aid-jbm13>3.0.Co;2-j.

98. Kligman S, Ren Z, Chung CH, Perillo MA, Chang YC, Koo H, Zheng Z, Li CS. The Impact of Dental Implant Surface Modifications on Osseointegration and Biofilm Formation. J Clin Med. 2021;10(8). doi:10.3390/jcm10081641.

99. Elias CN, Oshida Y, Lima JHC, Muller CA. Relationship between surface properties (roughness, wettability and morphology) of titanium and dental implant removal torque. J Mech Behav Biomed Mater. 2008;1(3):234-42. doi:10.1016/j.jmbbm.2007.12.002.

100. Koppány F, Csomó KB, Varmuzsa EM, Bognár E, Pelyhe L, Nagy P, Kientzl I, Szabó D, Weszl M, Dobos G, Lenk S, Erdei G, Kiss G, Nagy L, Sréter A, Belik AA, Tóth Z, Vág J, Joób-Fancsaly Á, Németh Z. Enhancement of Hydrophilicity of Nano-Pitted TiO(2) Surface Using Phosphoric Acid Etching. Nanomaterials (Basel). 2023;13(3). doi:10.3390/nano13030511.

101. Roth TA, Suppayak P. The surface and grain boundary free energies of pure titanium and the titanium alloy Ti□6Al□4V. Mater Sci Eng. 1978;35(2):187-96. doi:10.1016/0025-5416(78)90120-9.

102. Guillemot F, Porté MC, Labrugère C, Baquey C. Ti4+ to Ti3+ conversion of TiO2 uppermost layer by low-temperature vacuum annealing: interest for titanium biomedical applications. J Colloid Interface Sci. 2002;255(1):75-8. doi:10.1006/jcis.2002.8623.

103. Chauhan P, Koul V, Bhatnagar N. Critical role of etching parameters in the evolution of nano micro SLA surface on the Ti6Al4V alloy dental implants. Materials. 2021;14(21). doi:10.3390/ma14216344.

104. Tal-Gutelmacher E, Eliezer D. The hydrogen embrittlement of titanium-based alloys. JOM. 2005;57(9):46-9. doi:10.1007/s11837-005-0115-0.

105. Park JW, Kim YJ, Jang JH, Kwon TG, Bae YC, Suh JY. Effects of phosphoric acid treatment of titanium surfaces on surface properties, osteoblast response and removal of torque forces. Acta Biomater. 2010;6(4):1661-70. doi:10.1016/j.actbio.2009.10.011.

106. Prando D, Brenna A, Diamanti MV, Beretta S, Bolzoni F, Ormellese M, Pedeferri M. Corrosion of titanium: part 1: aggressive environments and main forms of degradation. J Appl Biomater Funct Mater. 2017;15(4):e291-e302. doi:10.5301/jabfm.5000387.

107. Jiang P, Zhang Y, Hu R, Shi B, Zhang L, Huang Q, Yang Y, Tang P, Lin C. Advanced surface engineering of titanium materials for biomedical applications: From static modification to dynamic responsive regulation. Bioact Mater. 2023;27:15-57. doi:10.1016/j.bioactmat.2023.03.006.

108. Lin X, Zhou L, Li S, Lu H, Ding X. Behavior of acid etching on titanium: topography, hydrophility and hydrogen concentration. Biomed Mater. 2014;9(1):015002. doi:10.1088/1748-6041/9/1/015002.

109. Linklater DP, Baulin VA, Juodkazis S, Crawford RJ, Stoodley P, Ivanova EP. Mechano-bactericidal actions of nanostructured surfaces. Nat Rev Microbiol. 2021;19(1):8-22. doi:10.1038/s41579-020-0414-z.

110. Wennerberg A, Albrektsson T. Effects of titanium surface topography on bone integration: a systematic review. Clin Oral Implants Res. 2009;20 Suppl 4:172-84. doi:10.1111/j.1600-0501.2009.01775.x.

111. Sotgiu G, Orsini M, Porcelli F, De Santis S, Petrucci E. Wettability of micro and nanostructured surface of titanium based electrodes: Influence of chemical and electrochemical etching. Chemical Engineering Transactions. 2021;86:1417-22.

112. Cheng S, Lee J-C. Acidity and catalytic activity of phosphoric acid modified titanium oxide surface. J Chin Chem Soc. 1988;35(3):191-8. doi:10.1002/jccs.198800028.

113. Wang Z, Mahmood A, Xie X, Wang X, Qiu H, Sun J. Surface adsorption configurations of H3PO4 modified TiO2 and its influence on the photodegradation intermediates of gaseous o-xylene. Chem Eng J. 2020;393:124723.

114. Connor P, McQuillan AJ. Phosphate adsorption onto TiO2 from aqueous solutions: an in situ internal reflection infrared spectroscopic study. Langmuir. 1999;15(8):2916-21.

115. Holmberg JP, Ahlberg E, Bergenholtz J, Hassellöv M, Abbas Z. Surface charge and interfacial potential of titanium dioxide nanoparticles: Experimental and theoretical investigations. J Colloid Interface Sci. 2013;407:168-76.

116. Coelho PG, Granjeiro JM, Romanos GE, Suzuki M, Silva NRF, Cardaropoli G, Thompson VP, Lemons JE. Basic research methods and current trends of dental implant surfaces. J Biomed Mater Res B Appl Biomater. 2009;88B(2):579-96. doi:10.1002/jbm.b.31264.

117. Doi K, Abe Y, Kobatake R, Okazaki Y, Oki Y, Naito Y, Prananingrum W, Tsuga K. Novel development of phosphate treated porous hydroxyapatite. Materials (Basel). 2017;10(12). doi:10.3390/ma10121405.

118. Rupp F, Liang L, Geis-Gerstorfer J, Scheideler L, Hüttig F. Surface characteristics of dental implants: A review. Dent Mater. 2018;34(1):40-57. doi:10.1016/j.dental.2017.09.007.

119. Rupp F, Scheideler L, Eichler M, Geis-Gerstorfer J. Wetting behavior of dental implants. Int J Oral Maxillofac Implants. 2011;26(6):1256-66.

120. Rupp F, Scheideler L, Olshanska N, de Wild M, Wieland M, Geis-Gerstorfer J. Enhancing surface free energy and hydrophilicity through chemical modification of

microstructured titanium implant surfaces. J Biomed Mater Res A. 2006;76A(2):323-34. doi:10.1002/jbm.a.30518.

121. Park JY. How titanium dioxide cleans itself. Science. 2018;361(6404):753. doi:10.1126/science.aau6016.

122. Ueno T, Takeuchi M, Hori N, Iwasa F, Minamikawa H, Igarashi Y, Anpo M, Ogawa T. Gamma ray treatment enhances bioactivity and osseointegration capability of titanium. J Biomed Mater Res B Appl Biomater. 2012;100(8):2279-87. doi:10.1002/jbm.b.32799.

123. Amini M, Majles Ara MH. Changes in structural and optical properties due to γ-irradiation of MgO nanoparticles. Radiochimica Acta. 2020;108(4):315-20.

124. Vu DKN, Nguyen DKV. Gamma irradiation-assisted synthesis of silver nanoparticle-embedded graphene oxide-TiO2 nanotube nanocomposite for organic dye photodegradation. J Nanomater. 2021;2021:1-14.

125. Toffoli A, Parisi L, Tatti R, Lorenzi A, Verucchi R, Manfredi E, Lumetti S, Macaluso GM. Thermal-induced hydrophilicity enhancement of titanium dental implant surfaces. J Oral Sci. 2020;62(2):217-21. doi:10.2334/josnusd.19-0235.

126. Lee YJ, Cui DZ, Jeon HR, Chung HJ, Park YJ, Kim OS, Kim YJ. Surface characteristics of thermally treated titanium surfaces. J Periodontal Implant Sci. 2012;42(3):81-7. doi:10.5051/jpis.2012.42.3.81.

127. Lee JH, Ogawa T. The biological aging of titanium implants. Implant Dent. 2012;21(5):415-21. doi:10.1097/ID.0b013e31826a51f4.

9. BIBLIOGRAPHY OF THE CANDIDATE'S RELATED PUBLICATIONS

1. Koppány F, Csomó KB, Varmuzsa EM, Bognár E, Pelyhe L, Nagy P, Kientzl I, Szabó D, Weszl M, Dobos G, Lenk S, Erdei G, Kiss G, Nagy L, Sréter A, Belik AA, Tóth Z, Vág J, Joób-Fancsaly Á, Németh Z. Enhancement of Hydrophilicity of Nano-Pitted TiO(2) Surface Using Phosphoric Acid Etching. Nanomaterials (Basel). 2023;13(3).

2. Koppány F. A fogászati implantátumok felületmorfológiájának befolyása a csontintegrációra. Fogorv Sz. 2019;112(1):18-23.

3. Koppány F, Bérczy K, Körmöczi K, Németh Z. [Changes in the "classical" factors influencing dental implant-osseointegration in recent decades]. Orv Hetil. 2019;160(37):1455-63.

10. ACKNOWLEDGEMENTS

First and foremost, I would like to thank my supervisor, Prof. Dr. Zsolt Németh, for his extraordinary patience, support, and guidance throughout my work.

I would like to express my gratitude to Dr. Eszter Bognár, Dr. Imre Kientzl, and Miklós Weszl, as well as Liza Pelyhe, for allowing me to delve into the world of nanostructured surfaces and for providing material and scientific guidance that fundamentally shaped my work. I also owe them thanks for introducing me to the nano-pitted surface and its production possibilities.

I am grateful to Gábor Kiss, Gábor Lenk, and Gábor Erdei for their assistance with the investigative methods, the implementation of measurements, and the statistical analysis.

I would also like to thank my friend, Dr. Krisztián Csomó, who has been one of the driving forces behind my scientific research. His ideas and thoughts have laid the foundation for our innovative efforts. I am also thankful to his wife, Dr. Andrea Belik, for her insights and excellent English language skills, which have always been of great help to me. Without them, this work could not have been completed.

I would like to thank Dr. Lilien Nagy and Dr. Márton Varmuzsa for their dedicated work in both the preparation of samples and the measurements.

Over the years of my work and studies, this thesis would not have been realized without the support and collaboration of the following individuals: Dr. Zsuzsanna Tóth, Prof. Dr. János Vág, Dr. Péter Nagy, and Dániel Szabó.

I owe long-standing gratitude to Prof. Dr. György Szabó, who was of great assistance during my PhD studies and the preparation of my scientific papers, and to Prof. Dr. Tamás Divinyi, on whom I could always rely for both professional and fatherly advice.

I would also like to express my special thanks to Dr. Kinga Körmöczi and all my colleagues who stood by me when I needed help.

Last but not least, I would like to thank my friend, Dr. Árpád Joób-Fancsaly, for his support and encouragement in my career advancement. He drew my attention to the possibilities of acid etching. He has always supported me, and I regard him as a role model in both scientific perseverance and humanity.